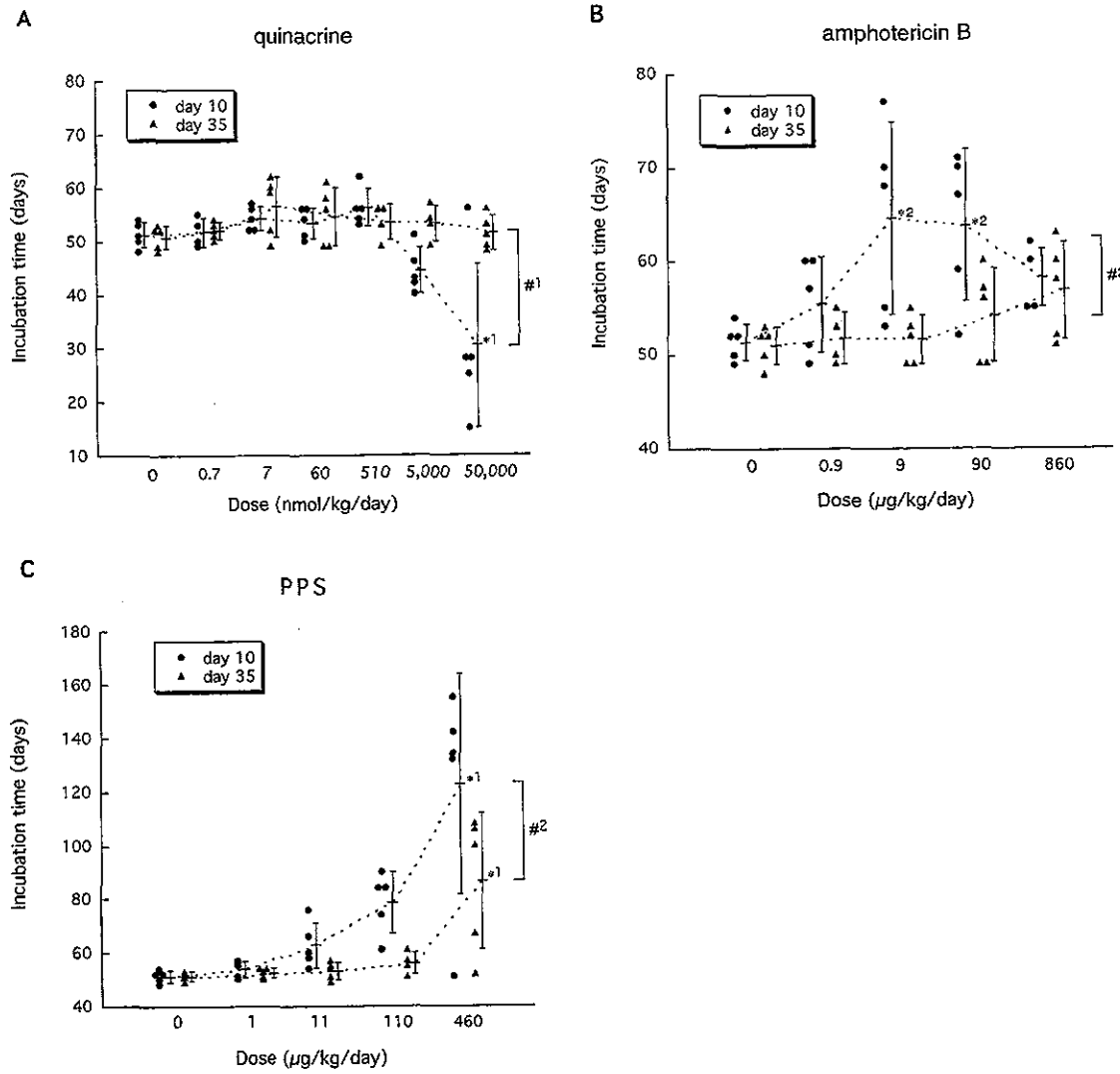


FIG. 1. Efficacy of quinacrine (A), amphotericin B (B), and PPS (C) in intracerebrally infected mice. Intraventricular infusion of a chemical was initiated at an early infection stage (day 10 postinoculation) or at a late stage (day 35) in 263K-infected Tg7 mice and continued for 4 weeks. Each circle or triangle represents an individual mouse. Bars represent the means and standard deviations of the incubation times for each group. *1, $P < 0.05$ versus the neighboring group and $P < 0.01$ versus the other groups; *2, $P < 0.05$ versus the vehicle control; #1, $P < 0.05$, #2, $P < 0.01$.

fur and bradykinesia on the day before or the day of death. The incubation period during which the animals were observed every day lasted from the time of intracerebral infection to the time of an obvious clinical stage.

Tga20 mice (14), which overexpress mouse PrP, were similarly inoculated with 1% RML agent mouse homogenate or 1% Fukuoka-1 agent mouse homogenate, and 4-week continuous intraventricular infusion of a chemical was started at day 14 or 49 postinoculation as described above.

**Chemicals.** The E-64d cysteine protease inhibitor was generously provided by S. Ishiura, Tokyo University, Tokyo, Japan. Quinacrine and chloroquine were obtained from Sigma. Amphotericin B (Fungizone) was purchased from Bristol-Myers Squibb (Tokyo, Japan). The sodium salt of PPS (Cartrophen Vet) was purchased from Biopharm (Bondi Junction, New South Wales, Australia) and used after removal of an alcohol additive by drying. E-64d was dissolved in dimethyl sulfoxide, amphotericin B was dissolved in distilled water, and all other chemicals were dissolved in phosphate-buffered saline (PBS).

**Immunohistochemistry, immunoblotting, and infectivity assay.** Mouse brains were fixed with 10% formalin and embedded in paraffin. Sections (5 μm thick) of the coronal slice sited around one-third of the distance from the interaural line to the bregma line were dewaxed and immunostained with an anti-PrP-C antibody (1:200; Immuno-Biological Labs, Gunma, Japan) or an antibody against glial fibrillary acidic protein (GFAP) (1:1,000; Dako, Glostrup, Denmark) as previously described (11).

For the detection of protease-resistant PrP (PrPres) by immunoblotting, the whole brain hemisphere where the intraventricular cannula had been fitted was homogenized with a ninefold volume of lysis buffer (0.5% sodium deoxycholate, 0.5% Nonidet P-40, PBS), and following low-speed centrifugation, the supernatant (Sup1) was treated with 25 μg of proteinase K per ml for 30 min at 37°C. An aliquot corresponding to 2.0 mg of brain tissue was electrophoresed in a sodium dodecyl sulfate–15% polyacrylamide gel and electroblotted onto a polyvinylidene difluoride filter. The filter was incubated with an anti-PrP-2B antibody raised against a hamster PrP fragment (amino acids 89 to 103) and then with an alkaline phosphatase-conjugated secondary antibody (Promega). Signals were visualized with CDP-Star detection reagent (Amersham).

For the infectivity assay, an aliquot of the Sup1 described above was diluted with PBS to produce a 0.1% brain homogenate, and a 20-μl aliquot of this homogenate was then inoculated intracerebrally in Tg7 mice. The infectious titer was calculated from the incubation period based on standard data obtained from an inoculation study with serially diluted homogenate samples of 263K-infected, terminally diseased brain tissue.

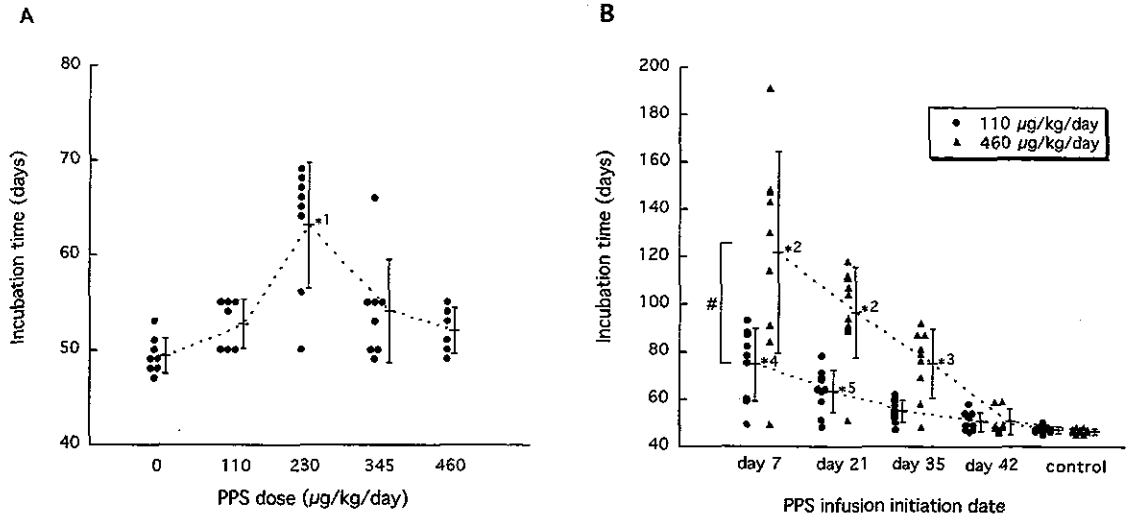


FIG. 2. Dose response (A) and administration timing (B) in PPS efficacy. Intraventricular infusion at the indicated concentrations (A) or at 110 or 460 μg/kg/day (B) was initiated at day 42 postinoculation (A) or at the indicated times (B) in intracerebrally 263K-infected Tg7 mice. *1, $P < 0.01$ versus the other groups; *2, $P < 0.01$ versus the other groups except the neighboring group(s); *3, $P < 0.05$ versus the control; *4, $P < 0.05$ versus the neighboring group and $P < 0.01$ versus the other groups; *5, $P < 0.01$ versus the control; #, $P < 0.01$.

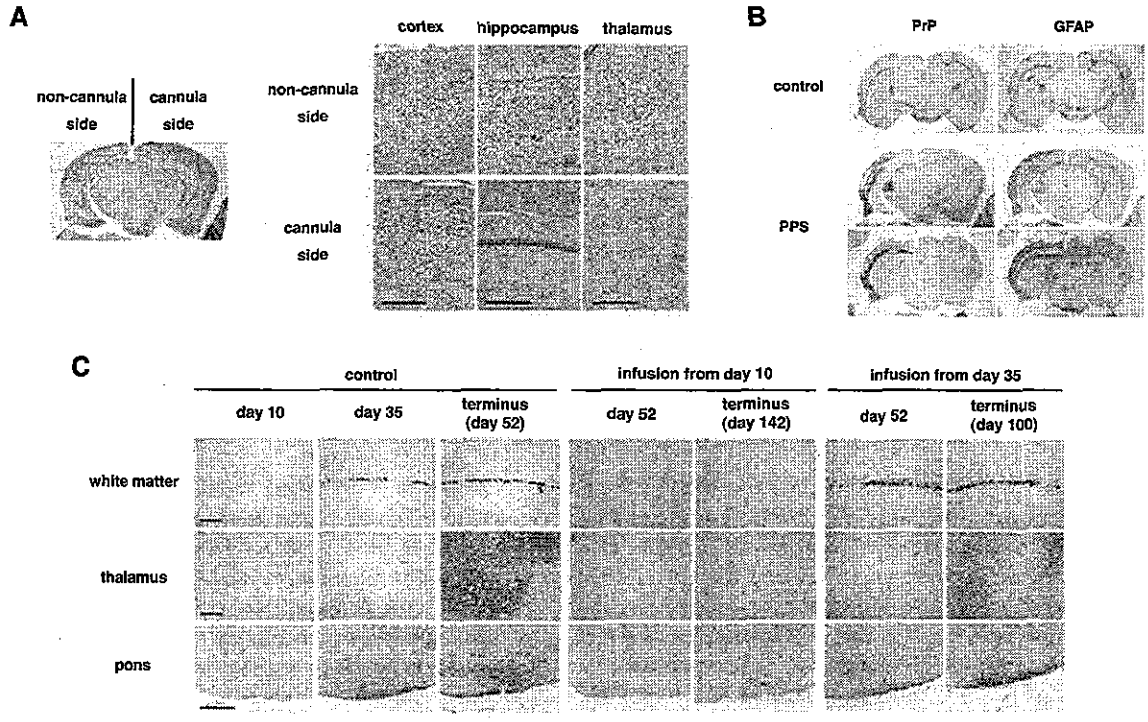


FIG. 3. Histopathology of the brain with or without PPS treatment. (A) Histology of the brain from an intracerebrally 263K-infected, long-surviving mouse treated with PPS at 460 μg/kg/day from day 10 postinoculation. Noncannula side and cannula side represent the sides of pathogen inoculation and intraventricular cannula implantation, respectively. Hematoxylin-eosin staining was used. (B) Immunohistochemical detection of abnormal PrP deposition (PrP) and of neurodegenerative changes by means of glial reaction (GFAP) in the same brain as for panel A (PPS) or in the brain from a nontreated mouse (control). The orientation of the sides of pathogen inoculation and cannula implantation is the same as in panel A. A coronal section sited around one-third of the distance from the interaural line to the bregma line is shown for the control mouse, and either a coronal section sited around one-third of the distance or a coronal section sited around two-thirds of the distance from the interaural line to the bregma line is shown for the PPS-treated mouse. Astrocytic glial reaction is demonstrated by immunohistochemistry for GFAP. (C) Sequential analysis of abnormal PrP deposition in intracerebrally 263K-infected, nontreated mice (control) or mice treated with PPS (infusion from day 10 or 35). Each panel shows a representative finding from three mice sacrificed at a designated time. In PPS-treated mice, the brain tissue examined was obtained from the hemisphere implanted with the intraventricular cannula, which was the hemisphere opposite to that of the inoculation site. PPS was infused at 460 μg/kg/day from day 10 or 35 postinoculation. Each image of the hippocampus or the thalamus (posterior nuclei) is from coronal sections sited around one-third of the distance from the interaural line to the bregma line. Each image of the pons (ventral area) is from a coronal section which is parallel to the interaural line and contains the culmen portion of the cerebellum. Bar, 160 μm.

**Safety assessment of PPS.** After reference to the Japanese national guidelines for safety studies on medicinal products (rodent and nonrodent toxicity testing), continuous 2-month PPS infusions ranging from 110 to 460 μg/kg/day were performed on each of four to seven adult mongrel dogs, Wistar rats, and Tg7 mice, using an Alzet osmotic pump and a brain infusion cannula. The blood cell count, coagulation, and serum chemistry were analyzed before PPS infusion was initiated and then each month thereafter. An electroencephalogram and 48-h spontaneous activity were recorded for the rats every 2 weeks from the time PPS infusion was started. Animals were sacrificed under deep anesthesia for histological evaluation of the brain when they reached an incurable condition or after the infusion had finished. Animal handling and sacrifice were in accordance with the national prescribed guidelines, and ethical approval for the studies was granted by the Animal Experiment Committee of Kyushu University.

***Statistical analysis.*** Statistical significance was analyzed by repeated-measure analysis of variance followed by Scheffé's method for multiple comparisons.

## RESULTS

**Vehicle control.** Inoculation-related accidental death occurred within 1 week of postintracerebral inoculation and abnormal PrP deposition in the brain appeared at around day 35 postinoculation in Tg7 mice intracerebrally inoculated with 1% 263K homogenate. Accordingly, intraventricular infusion of a chemical was initiated either at an early stage (day 10) or at a late stage (day 35) of the infection in Tg7 mice. Continuous 4-week intraventricular infusion with vehicle alone from day 10 or 35 did not alter the mean incubation time (distilled water, 51.6 ± 1.8 days [$n$ = 5] from day 10 and 51.0 ± 1.8 days [$n$ = 5] from day 35; 25% dimethyl sulfoxide, 52.3 ± 2.1 days [$n$ = 5] from day 10 and 51.2 ± 1.3 days [$n$ = 5] from day 35; untreated, 51.8 ± 2.2 days [$n$ = 8]).

**Antimalarial drugs, cysteine protease inhibitor, and amphotericin B.** Quinacrine (Fig. 1A), chloroquine (data not shown), and the E-64d cysteine protease inhibitor (data not shown) gave no prolongation effects. Overdose of quinacrine at more than 5 μmol/kg/day from day 10, however, caused adverse effects and shortened the incubation period. Amphotericin B prolonged the incubation time at a dose of 9 or 90 μg/kg/day from day 10 and gave about 26% prolongation of the mean incubation time (from 51 to 64 days) (Fig. 1B). With infusion from day 35, however, no significant prolongation was observed.

**PPS.** PPS showed the greatest beneficial effects among all of the chemicals examined in this study (Fig. 1C). Infusion at 460 μg/kg/day from day 10 gave 141% prolongation (from 51 to 123 days), and even from the late stage (day 35), it gave 71% prolongation (from 51 days to 87 days).

The dose response of PPS was further examined at a later stage of the infection, day 42 (Fig. 2A). The dose response was in a bell-shaped distribution, and the maximal effect was observed at a dose of 230 μg/kg/day, when the mean incubation time was prolonged by 29% (from 49 to 63 days).

The influence of infusion laterality on the outcome was examined by either ipsilateral or contralateral PPS administration to the inoculation site from day 10 or 35 postinoculation, but no significant difference according to the side of the infusion was observed (data not shown).

The relationship between the infusion initiation time and the outcome was analyzed (Fig. 2B). The effects of PPS were inversely correlated with time after inoculation. High-dose PPS infusion (460 μg/kg/day) at day 7 postinoculation prolonged the mean incubation period by 160% (from 47 to 122 days),

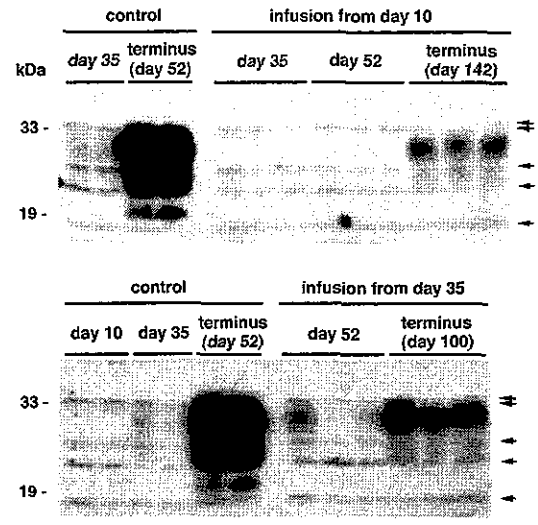


FIG. 4. PrPres in the brain with or without PPS treatment. Each lane represents an aliquot corresponding to 2.0 mg of brain tissue homogenate from an individual mouse sacrificed at a designated time. The brain tissue homogenate examined was prepared from the whole hemisphere contralateral to that of the inoculation site in either nontreated mice (control) or PPS-treated mice (infusion from day 10 or 35). In PPS-treated mice, the brain hemisphere examined was the side implanted with the intraventricular cannula. PPS was infused at 460 μg/kg/day from day 10 or 35 postinoculation. Nonspecific signals that were observed without the primary antibody are shown by arrows.

while that at day 21 postinoculation prolonged it by 106% (from 47 to 97 days). Low-dose PPS infusion (110 μg/kg/day) showed a similar pattern but was less effective.

As a supplementary experiment to compare the efficacy of intraventricular administration with that of peripheral administration, 4-week continuous PPS infusion at 0.2, 2 or 20 mg/kg/day into a subcutaneous area of the back was performed with an osmotic pump from day 10 or 35 postinoculation. None of these treatments yielded any statistically significant effectiveness in prolonging the incubation time (51.0 ± 1.8 days [$n$ = 4], 52.1 ± 2.1 days [$n$ = 4], 52.3 ± 1.6 days [$n$ = 5], and 23.8 ± 16.5 days [$n$ = 5] in the mice receiving 0, 0.2, 2, and 20 mg/kg/day from day 10, respectively; 51.8 ± 2.0 days [$n$ = 4], 51.0 ± 1.8 days [$n$ = 4], 50.0 ± 1.3 days [$n$ = 5], and 40.4 ± 4.3 days [$n$ = 5] in the mice receiving 0, 0.2, 2, and 20 mg/kg/day from day 35, respectively). However, treatment with the highest dose showed adverse effects, such as hemorrhage in the subcutaneous area surrounding the osmotic pump in 80% of the mice examined.

**PrP deposition and pathology.** Modification of abnormal PrP deposition and pathology in the brains of PPS-treated mice were analyzed (Fig. 3A and B). In the PPS-treated mice with an incubation period of 142 days, the brain hemisphere implanted with the PPS infusion cannula showed very faint or mild pathological changes, whereas the contralateral brain hemisphere was microscopically atrophied and accompanied by prominent spongiform degeneration and neuronal cell loss, especially in the cerebral cortex, hippocampus, and thalamus (Fig. 3A). Similarly, abnormal PrP deposition was prominently reduced within the brain hemisphere implanted with the infusion cannula, while abnormal PrP deposition was much en-

TABLE 1. Infectious titer and incubation time in the 263K-Tg7 model

| Dilution | Mean incubation time[a] (days) ± SD | No. of diseased mice/total | Infectious titer[b] (log $LD_{50}$/20 μl of tissue) | Corrected titer (log $LD_{50}$/g of tissue) |
|---|---|---|---|---|
| $10^1$ | 43.8 ± 2.5 | 9/9 | 6.3 | 8.0 |
| $10^2$ | 48.4 ± 3.1 | 10/10 | 5.3 | 7.0 |
| $10^3$ | 55.6 ± 5.3 | 9/9 | 4.3 | 6.0 |
| $10^4$ | 65.1 ± 2.9 | 8/8 | 3.3 | 5.0 |
| $10^5$ | 76.0 ± 5.3 | 8/8 | 2.3 | 4.0 |
| $10^6$ | 93.9 ± 17.0 | 10/10 | 1.3 | 3.0 |
| $10^7$ | 158, 177, 422, 443 | 4/8 | 0.3 | 2.0 |
| $10^8$ | 338, 555 | 2/7 | | |
| $10^9$ | | 0/9 | | |

[a] A 20-μl aliquot of serially diluted homogenate samples of the whole brain from a 263K-infected, terminally diseased Tg7 mouse was inoculated intracerebrally into Tg7 mice, and the mice were observed for up to 730 days postinoculation.
[b] The infectious titer was calculated by the Behrens-Kärber method.

hanced within the contralateral hemisphere, compared to the control mice with an incubation period of 52 days (Fig. 3B). GFAP immunoreactivity, indicating glial reaction, was similar to the PrP deposition.

In a sequential analysis of the control mice, cerebral PrP deposition had not appeared at day 10, first appeared in the cerebral white matter adjacent to the hippocampus at around day 35 in a coarse granular deposition pattern, and finally appeared in the thalamus, hypothalamus, and brain stem at terminus day 52 in a punctate pattern (Fig. 3C). Mice treated with PPS from day 10 did not show any PrP deposition within the hemisphere implanted with the cannula at day 52, and only punctate PrP deposition was observed in the brain stem at terminus day 142. Mice treated with PPS from day 35 demonstrated coarse granular PrP deposits in the cerebral white matter at day 52 within the cannula-implanted hemisphere, but there was no apparent PrP deposition in the thalamus at this stage. This PrP deposition pattern was similar to that in the control mice at day 35. Punctate PrP deposition was finally clearly visible in both the thalamus and the brain stem at terminus day 100.

**PrPres and infectivity.** PrPres was analyzed within the brain hemisphere implanted with the infusion cannula (Fig. 4). PrPres signals in the control mice were very faint at day 35 but ultimately were very strong at terminus day 52. In mice treated with PPS from day 10, PrPres signals were not detected in the brain at day 35 or 52 but were detected at terminus day 142. However, the PrPres signals at day 142 did not reach the high level seen in the control mice at day 52. Similarly, in mice treated with PPS from day 35, the PrPres signals were very weak at day 52 and then increased at terminus day 100, but they still remained at a lower level than in the control mice.

Modification of the infectivity within the brain hemisphere implanted with the infusion cannula was clearly correlated with the level of PrPres (Tables 1 and 2). The infectious titer (log 50% lethal dose [$LD_{50}$]/g of tissue) within the cannula-implanted brain hemisphere from terminally diseased mice was significantly decreased in the PPS-treated mice.

**PPS effects in other strains.** To investigate the effectiveness of PPS on pathogen strains other than 263K scrapie agent, Tga20 mice intracerebrally infected with 1% homogenates of RML scrapie agent or Fukuoka-1 Gerstmann-Sträussler-Scheinker disease agent were treated with a dose of 230 μg/kg/day for 4 weeks (Fig. 5). RML-infected mice treated with vehicle alone had a mean incubation period of 65 days, while those treated with PPS from day 14 or 49 postinoculation had a mean incubation period of 141 days (117% prolongation) or 95 days (46%), respectively. Similarly, Fukuoka-1-infected mice had a mean incubation period of 106 days, while those treated with PPS from day 14 or 49 postinoculation had a mean incubation period of 153 days (44% prolongation) or 133 days (25%), respectively. These data imply that intraventricular PPS infusion can be effective irrespective of the pathogen strain.

**Safety assessment of intraventricular PPS.** Thrombocytopenia and coagulation abnormality are known to occur occasionally with PPS, and PPS has been utilized in humans enterally, percutaneously, or intravenously but never intraventricularly. Thus, the safety of continuous intraventricular infusion should be evaluated before the possibility of application of this specific treatment to human patients is discussed. Continuous intraventricular infusion at doses ranging from 110 to 460 μg/kg/day was examined for 2 months in rodents (mice and rats) and nonrodents (dogs). Intraventricular infusion of up to

TABLE 2. Infectious titer in the brain with PPS treatment

| Inoculum[a] | Mouse no. | Mean incubation time[b] (days) ± SD | Infectious titer[c] (log $LD_{50}$/g of tissue) | Mean infectious titer ± SD[d] |
|---|---|---|---|---|
| Control | 1 | 56.4 ± 0.5 | 8.9 | 8.87 ± 0.06* |
| | 2 | 56.4 ± 1.6 | 8.9 | |
| | 3 | 57.2 ± 1.9 | 8.8 | |
| PPS from: | | | | |
| Day 35 postinoculation | 1 | 62.4 ± 1.2 | 8.3 | 8.20 ± 0.10* |
| | 2 | 63.4 ± 0.8 | 8.2 | |
| | 3 | 64.2 ± 5.6 | 8.1 | |
| Day 10 postinoculation | 1 | 69.8 ± 1.6 | 7.6 | 7.50 ± 0.14* |
| | 2 | 71.4 ± 1.5 | 7.4 | |

[a] A 20-μl aliquot of a 0.1% homogenate from the infusion cannula-implanted brain hemisphere of each terminally diseased mouse was used for intracerebral inoculation into Tg7 mice.
[b] The data were collected from five inoculated mice in each group.
[c] The infectious titer was calculated from the incubation period based on the curve obtained from the data in Table 1 and corrected for the dilution power.
[d] *, $P < 0.01$ versus the other groups.

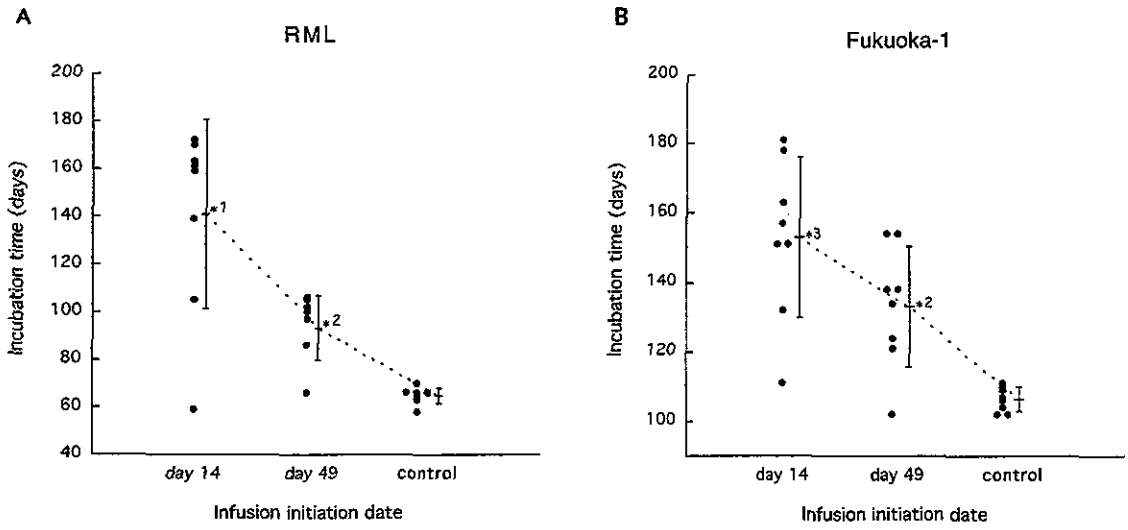


FIG. 5. Efficacy of PPS in mice infected with RML agent (A) or Fukuoka-1 agent (B). PPS at a dose of 230 μg/kg/day was intraventricularly infused into intracerebrally infected Tga20 mice from day 14 or 49 postinoculation for 4 weeks. *1, $P < 0.01$ versus the other groups; *2, $P < 0.05$ versus the control; *3, $P < 0.01$ versus the control.

230 μg/kg/day did not influence the data for the blood cell count, coagulation (Fig. 6), or serum chemistry, nor did it influence the electroencephalogram records, spontaneous activity pattern, behavior, or histological findings for the brain. However, higher doses showed adverse effects, but only in dogs. Three of the six dogs receiving 345 μg/kg/day and all four dogs receiving 460 μg/kg/day suffered partial or generalized seizures, which began within 24 h after PPS infusion was initiated. After treatment with anticonvulsants, the seizures of one dog from each group disappeared. The remaining five dogs did not recover from the seizures. Histologically, three of the five dogs had a large hematoma in the cerebral white matter where the cannula had been placed. None of the other dogs showed any notable pathological findings except for localized tissue damage and gliosis around the cannula route (data not shown).

## DISCUSSION

Here, we report on the effectiveness of clinically applicable chemicals by using a new drug evaluation system composed of gene-manipulated mice with substantially shorter disease incubation times and a continuous intraventricular infusion device. This system enabled us to evaluate the absolute therapeutic potency of chemicals in vivo within relatively short periods, regardless of their accessibility to the brain. Our observations indicate that two of the chemicals examined were effective in prolonging the incubation periods for intracerebrally infected animals. This suggests that intraventricular drug infusion could improve the prognosis of infected humans.

Among the chemicals examined here, PPS showed the most beneficial effects, and despite a limited infusion period, mice treated with PPS survived long after the infusion ended. Effectiveness was clearly observed even for the infusion at a late stage of infection, when abnormal PrP deposition was already visible in the affected brain. PPS is known to be effective in inhibiting abnormal PrP formation in vitro (5) and/or in prolonging the disease incubation time in vivo (9, 12, 13, 16). However, its effectiveness in vivo has been restricted to administration either before or soon after peripheral infection. Thus, treatment with PPS has been thought of as being preventive only for those individuals with accidental inoculation in the periphery (7). Our observations, however, indicate that intraventricular PPS is in fact quite effective in prolonging the life spans of infected animals, even after abnormal PrP has already accumulated in the brain. The difference between previous observations and ours can be explained by poor or even no accessibility of peripherally administered PPS to the brain, and this is supported by our observation of the ineffectiveness of continuous subcutaneous PPS administration in intracerebrally infected mice.

The present studies revealed that PPS prevented not only new deposition of abnormal PrP but also the accumulation of neurodegeneration and infectivity. These findings suggest that prolongation of the life spans of infected animals by PPS could be due to its direct action on abnormal PrP generation. PPS interferes with the conversion of normal PrP molecules to abnormal ones by competitively binding to the PrP molecules (4, 5) and/or by altering the cellular localization of normal PrP molecules (20). PPS is also known to play a stimulatory role in the conversion of PrP molecules into protease-resistant ones in vitro (22). However, neither stimulatory effects on abnormal PrP accumulation nor acceleration of the disease course was observed in the present in vivo study.

From the histopathological studies, the effectiveness of PPS was clearly observed within the brain hemisphere where the intraventricular cannula was fitted, but not within the other hemisphere, in treated mice that survived long after the infusion had ended. This suggests that the infused PPS persisted around the infusion site and did not diffuse throughout the ventricular system, especially into the contralateral side of the brain. To obtain a much better outcome following PPS admin-

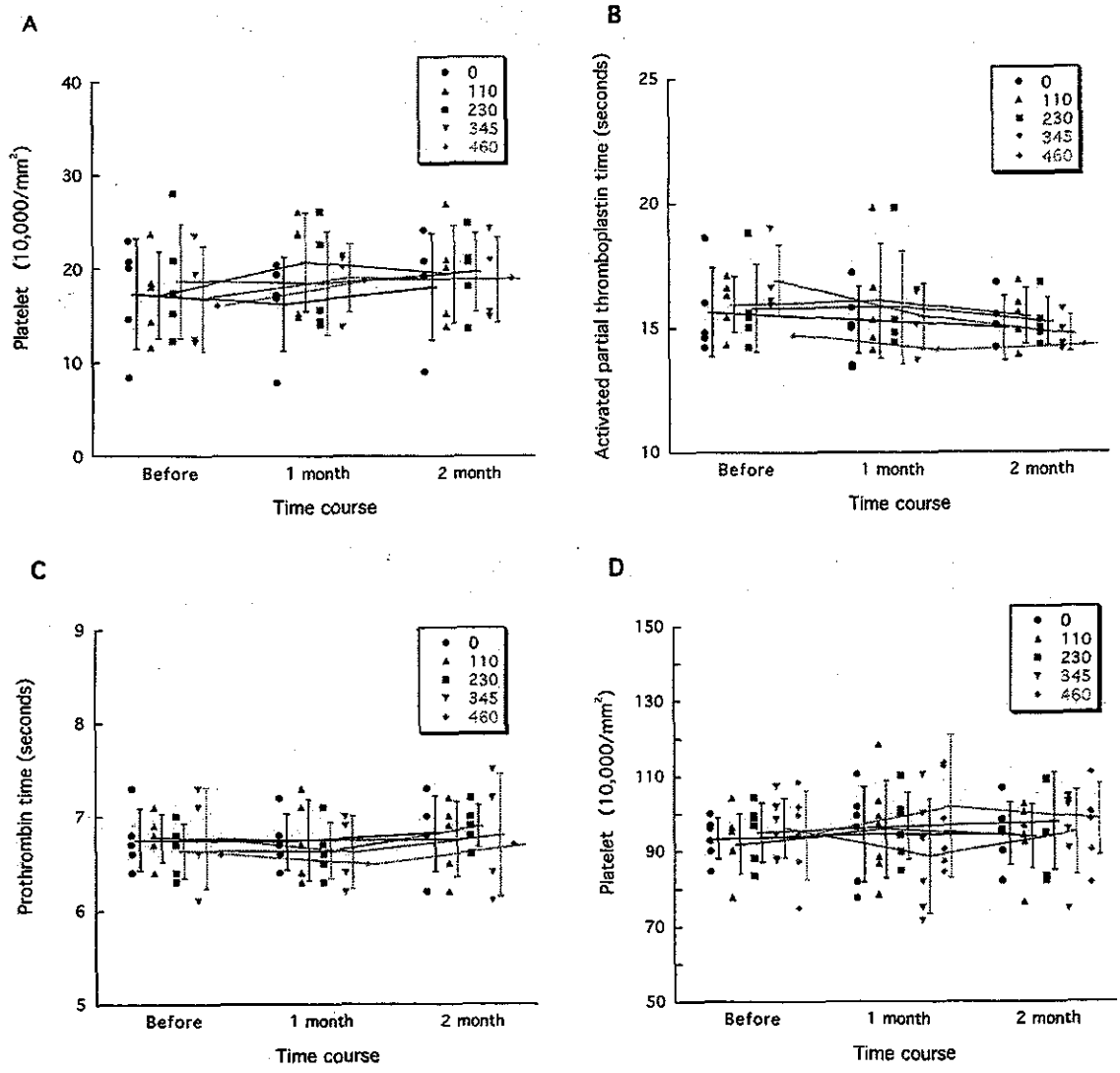


FIG. 6. Representative data from PPS safety assessment. Platelet counts in dogs and rats (A and D, respectively) and coagulation data for dogs (B and C) are shown. Each circle, triangle, square, inverted triangle, or diamond represents an individual animal. The data for two of the six dogs receiving 345 μg/kg/day and for three of the four dogs receiving 460 μg/kg/day were not obtained because they suffered seizures shortly after PPS infusion had been started and were sacrificed or died. However, the data for two dogs, one receiving 345 μg/kg/day and the other receiving 460 μg/kg/day, both of which suffered seizures but recovered, are included.

istration, it may be important to facilitate the diffuse distribution of PPS into every vulnerable area of the brain.

These studies also demonstrated that both the cerebral cortex and the hippocampus were apparently involved in the pathological conditions at the latest stage of the disease in the Tg7-263K model. Coarse granular PrP deposits in the cerebral white matter were the earliest abnormal finding in the affected brain, and these were followed by punctate PrP deposits in the brain stem, hypothalamus, and thalamus, but not in the cerebral cortex and hippocampus, in the nontreated mice. However, mice surviving long after intraventricular PPS infusion had devastating pathological changes in the cerebral cortex and hippocampus of the hemisphere opposite to that of the PPS infusion.

The PPS effects were quite dependent upon the timing of the infusion, and at a later disease stage or a terminal disease stage the effects on prolongation of the life span were substantially limited. We have no precise knowledge as to when the mice used began to exhibit the very initial signs or symptoms of the disease, although we do know that abnormal PrP deposition in the brain began to be visible at around 5 weeks postinoculation and that the mice started to show definite signs about 2 days before death. Thus, our data do not guarantee similar effectiveness in human patients who already have signs and symptoms of the disease. On the other hand, the effectiveness of intraventricular PPS infusion was demonstrated not only for infection with the 263K strain but also for infection with two other distinct strains. These findings suggest that this treatment may have universal validity for TSE diseases.

PPS is utilized as a clinical medicine for interstitial cystitis, thrombophlebitis, and thrombosis, and its safety by enteral, percutaneous or intravenous administration has been clearly

established. Here, the safety of intraventricular PPS infusion at up to a dose yielding the maximal effectiveness in mice was demonstrated in experimental animals. However, at higher doses than this, there was a gap between small rodents and dogs, with the dogs showing adverse effects, such as seizures that were mostly caused by hematoma formation around the intraventricular cannula, although such adverse effects appeared only very early in the treatment. It is well known that smaller animals metabolize drugs much more quickly, and therefore intraventricular PPS at the same dosage was not toxic in mice and rats but was toxic in dogs. For application of this treatment to humans, it will be important to take account of the drug metabolism differences between mice and humans.

Amphotericin B and one of its derivatives are known to prolong the life spans of infected animals even with administration late in the disease course (8). In our experiments, however, amphotericin B did not cause any significant prolongation at a late-stage administration. Differences in the administration route, dose, and duration, as well as the experimental models, might account for this difference, but it remains to be elucidated.

Antimalarial chemicals, including quinacrine, had no effects in the present studies. These chemicals were previously found to be effective in inhibiting abnormal PrP formation in a scrapie-infected cell line (10, 15), and quinacrine has been used in clinical trials for TSE patients. However, together with the recent findings of two other research groups (1, 6), our data suggest that quinacrine may not improve the prognosis of the patients.

Finally, the placement of an intraventricular cannula in TSE patients may create public health issues due to fears of contamination of the operating room or safety issues with respect to the personnel involved with this procedure. For these reasons, other drug delivery systems which do not need a surgical procedure should be developed, and PPS derivatives that can be delivered into the brain after peripheral administration also need to be developed. As an immediately applicable remedy, however, continuous intraventricular PPS administration with an infusion device may be a candidate for a clinical trial, with a view to preventing the disease in those people categorized as being at extremely high risk or to improving the prognosis of diseased people with TSEs.

## ACKNOWLEDGMENTS

This study was supported by grants to K.D. from the Ministry of Health, Labour and Welfare (H13-kokoro-025) and from the Ministry of Education, Culture, Sports, Science and Technology (13557118 and 14021085), Tokyo, Japan.

We thank B. Chesebro of the Rocky Mountain Laboratories, National Institute of Allergy and Infectious Diseases, National Institutes of Health, for providing the Tg7 mice and C. Weissmann of the Imperial College School of Medicine at St. Mary's, London, United Kingdom, for providing the Tga20 mice. We also thank I. Goto for the electroencephalogram analyses.

## REFERENCES

1. **Barret, A., F. Tagliavini, G. Forloni, C. Bate, M. Salmona, L. Colombo, A. De Luigi, L. Limido, S. Suardi, G. Rossi, F. Auvré, K. T. Adjou, N. Salés, A. Williams, C. Lasmézas, and J. P. Deslys.** 2003. Evaluation of quinacrine treatment for prion diseases. J. Virol. 77:8462–8469.
2. **Brown, P.** 2002. Drug therapy in human and experimental transmissible spongiform encephalopathy. Neurology 58:1720–1725.
3. **Brown, P., M. Preece, J. P. Brandel, T. Sato, L. McShane, I. Zerr, A. Fletcher, R. G. Will, M. Pocchiari, N. R. Cashman, J. H. d'Aignaux, L. Cervenakova, J. Fradkin, L. B. Schonberger, and S. J. Collins.** 2000. Iatrogenic Creutzfeldt-Jakob disease at the millennium. Neurology 55:1075–1081.
4. **Caughey, B., K. Brown, G. J. Raymond, G. E. Katzenstein, and W. Thresher.** 1994. Binding of the protease-sensitive form of PrP (prion protein) to sulfated glycosaminoglycan and Congo red. J. Virol. 68:2135–2141.
5. **Caughey, B., and G. J. Raymond.** 1993. Sulfated polyanion inhibition of scrapie-associated PrP accumulation in cultured cells. J. Virol. 67:643–650.
6. **Collins, S. J., V. Lewis, M. Brazier, A. F. Hill, A. Fletcher, and C. L. Masters.** 2002. Quinacrine does not prolong survival in a murine Creutzfeldt-Jakob disease model. Ann. Neurol. 52:503–506.
7. **Dealler, S.** 1998. Post-exposure prophylaxis after accidental prion inoculation. Lancet 351:600.
8. **Demaimay, R., K. T. Adjou, V. Beringue, S. Demart, C. I. Lasmézas, J. P. Deslys, M. Seman, and D. Dormont.** 1997. Late treatment with polyene antibiotics can prolong the survival time of scrapie-infected animals. J. Virol. 71:9685–9689.
9. **Diringer, H., and B. Ehlers.** 1991. Chemoprophylaxis of scrapie in mice. J. Gen. Virol. 72:457–460.
10. **Doh-ura, K., T. Iwaki, and B. Caughey.** 2000. Lysosomotropic agents and cysteine protease inhibitors inhibit scrapie-associated prion protein accumulation. J. Virol. 74:4894–4897.
11. **Doh-ura, K., E. Mekada, K. Ogomori, and T. Iwaki.** 2000. Enhanced CD9 expression in the mouse and human brains infected with transmissible spongiform encephalopathies. J. Neuropathol. Exp. Neurol. 59:774–785.
12. **Ehlers, B., and H. Diringer.** 1984. Dextran sulphate 500 delays and prevents mouse scrapie by impairment of agent replication in spleen. J. Gen. Virol. 65:1325–1330.
13. **Farquhar, C., A. Dickinson, and M. Bruce.** 1999. Prophylactic potential of pentosan polysulphate in transmissible spongiform encephalopathies. Lancet 353:117.
14. **Fischer, M., T. Rulicke, A. Raeber, A. Sailer, M. Moser, B. Oesch, S. Brandner, A. Aguzzi, and C. Weissmann.** 1996. Prion protein (PrP) with amino-proximal deletions restoring susceptibility of PrP knockout mice to scrapie. EMBO J. 15:1255–1264.
15. **Korth, C., B. C. May, F. E. Cohen, and S. B. Prusiner.** 2001. Acridine and phenothiazine derivatives as pharmacotherapeutics for prion disease. Proc. Natl. Acad. Sci. USA 98:9836–9841.
16. **Ladogana, A., P. Casaccia, L. Ingrosso, M. Cibati, M. Salvatore, Y. G. Xi, C. Masullo, and M. Pocchiari.** 1992. Sulphate polyanions prolong the incubation period of scrapie-infected hamsters. J. Gen. Virol. 73:661–665.
17. **Priola, S. A., B. Caughey, and W. S. Caughey.** 1999. Novel therapeutic uses for porphyrins and phthalocyanines in the transmissible spongiform encephalopathies. Curr. Opin. Microbiol. 2:563–566.
18. **Prusiner, S. B.** 1998. Prions. Proc. Natl. Acad. Sci. USA 95:13363–13383.
19. **Race, R. E., S. A. Priola, R. A. Bessen, D. Ernst, J. Dockter, G. F. Rall, L. Mucke, B. Chesebro, and M. B. Oldstone.** 1995. Neuron-specific expression of a hamster prion protein minigene in transgenic mice induces susceptibility to hamster scrapie agent. Neuron 15:1183–1191.
20. **Shyng, S. L., S. Lehmann, K. L. Moulder, and D. A. Harris.** 1995. Sulfated glycans stimulate endocytosis of the cellular isoform of the prion protein, PrPC, in cultured cells. J. Biol. Chem. 270:30221–30229.
21. **Will, R. G., J. W. Ironside, M. Zeidler, S. N. Cousens, K. Estibeiro, A. Alperovitch, S. Poser, M. Pocchiari, A. Hofman, and P. G. Smith.** 1996. A new variant of Creutzfeldt-Jakob disease in the UK. Lancet 347:921–925.
22. **Wong, C., L. W. Xiong, M. Horiuchi, L. Raymond, K. Wehrly, B. Chesebro, and B. Caughey.** 2001. Sulfated glycans and elevated temperature stimulate PrP(Sc)-dependent cell-free formation of protease-resistant prion protein. EMBO J. 20:377–386.

*Journal of General Virology* (2004), 85, 1785–1790 DOI 10.1099/vir.0.19754-0

# Amyloid imaging probes are useful for detection of prion plaques and treatment of transmissible spongiform encephalopathies

Kensuke Ishikawa,[1] Katsumi Doh-ura,[1]† Yukitsuka Kudo,[2] Noriyuki Nishida,[3] Ikuko Murakami-Kubo,[1] Yukio Ando,[4] Tohru Sawada[2] and Toru Iwaki[1]

[1]Department of Neuropathology, Neurological Institute, Graduate School of Medical Sciences, Kyushu University, 3-1-1 Maidashi, Higashi-ku, Fukuoka 812-8582, Japan

[2]BF Research Institute Inc., Osaka 565-0873, Japan

[3]Department of Bacteriology, Nagasaki University School of Medicine, Nagasaki, 852-8501, Japan

[4]Department of Laboratory Medicine, Kumamoto University, Kumamoto 860-0081, Japan

Correspondence
Kensuke Ishikawa
kensuke@np.med.kyushu-u.ac.jp
Katsumi Doh-ura
doh-ura@mail.tains.tohoku.ac.jp

Received 24 October 2003
Accepted 2 March 2004

Diagnostic imaging probes have been developed to monitor cerebral amyloid lesions in patients with neurodegenerative disorders. A thioflavin derivative, 2-[4′-(methylamino)phenyl] benzothiazole (BTA-1) and a Congo red derivative, (*trans*, *trans*),-1-bromo-2,5-bis-(3-hydroxycarbonyl-4-hydroxy)styrylbenzene (BSB) are representative chemicals of these probes. In this report, the two chemicals were studied in transmissible spongiform encephalopathies (TSE). Both BTA-1 and BSB selectively bound to compact plaques of prion protein (PrP), not only in the brain specimens of certain types of human TSE, but also in the brains of TSE-infected mice when the probes were injected intravenously. The chemicals bound to plaques in the brains were stable and could be detected for more than 42 h post-injection. In addition, the chemicals inhibited abnormal PrP formation in a cellular model of TSE with $IC_{50}$ values of 4 nM for BTA-1 and 1·4 μM for BSB. In an experimental mouse model, the intravenous injection of 1 mg BSB prolonged the incubation period by 14%. This efficacy was only observed against the RML strain and not the other strains examined. These observations suggest that these chemicals bind directly to PrP aggregates and inhibit new formation of abnormal PrP in a strain-dependent manner. Both BTA-1 and BSB can be expected to be lead chemicals not only for imaging probes but also for therapeutic drugs for TSEs caused by certain strains.

## INTRODUCTION

The transmissible spongiform encephalopathies (TSEs or prion diseases) form a group of fatal neurodegenerative diseases including bovine spongiform encephalopathy, Creutzfeldt–Jakob disease (CJD) and Gerstmann–Sträussler–Scheinker syndrome (GSS). These diseases are characterized by the accumulation in the brain of abnormal protease-resistant isoforms of prion protein (PrP), termed $PrP^{Sc}$ (Prusiner, 1991). The diseases are rare, but outbreaks of acquired forms of CJD, such as variant CJD (Will *et al.*, 1996) and iatrogenic CJD with cadaveric growth hormone or dura grafts (Hamad *et al.*, 2001), have prompted the development of therapeutic interventions and new diagnostic methods.

There are several drug candidates currently under clinical trial for TSE patients, but unfortunately their potential usefulness remains limited. The problem is that these agents can only be given after the onset of the disease, often in the advanced stage, because there is no reliable means of detecting presymptomatic infection by either neuroimaging or laboratory examination. Some studies have reported that imaging assessments such as positron emission tomography (PET) with [$^{18}$F]FDG and diffusion-weighted magnetic resonance imaging are useful for some types of human TSE (Demaerel *et al.*, 1997; Murata *et al.*, 2002), but are not always conclusive. At present, TSEs can be diagnosed with certainty only through pathological examination or immunoblotting of the diseased brain. Recently, PET and single photon emission CT (SPECT) using radiolabelled imaging probes, which provide information on neuropathological changes as well as brain metabolism, have been reported to be helpful for the early diagnosis of neurodegenerative disorders. A variety of chemicals have been evaluated for imaging β-amyloid (Aβ) aggregation, which is the major

†Present address: Department of Prion Research, Tohoku University Graduate School of Medicine, Sendai 980-8575, Japan.

hallmark of Alzheimer's disease. Candidate probes have primarily been derived from amyloid dyes such as thioflavin and Congo red (Bacskai *et al.*, 2002).

Here, we focused on two candidate probes: a thioflavin derivative, 2-[4'-(methylamino)phenyl] benzothiazole (BTA-1) and a Congo red derivative, (*trans, trans*),-1-bromo-2,5-bis-(3-hydroxycarbonyl-4-hydroxy)styrylbenzene (BSB) (Fig. 1). Both chemicals have been reported to detect amyloid or amyloid-like plaques in either post-mortem human brains or living mouse brains (Mathis *et al.*, 2002; Skovronsky *et al.*, 2000). Since $PrP^{Sc}$ tends to exist as amyloid-like fibrils, we used either BTA-1 or BSB to label PrP deposition in TSE brains. We also examined these chemicals for their application as therapeutics for TSE, since some amyloid-binding chemicals have the potential to inhibit $PrP^{Sc}$ propagation in *in vitro* and/or *in vivo* models of TSE (Supattapone *et al.*, 2002).

## METHODS

**Chemicals and experimental models.** BTA-1 was synthesized at Tanabe R & D (Saitama, Japan), and BSB was kindly provided by Dojindo Laboratories (Kumamoto, Japan). The chemicals were dissolved in 100% dimethylsulfoxide (DMSO) and stored at 4 °C until use.

Three kinds of TSE-infected mouse neuroblastoma (N2a) cell lines were used in this study: N2a cells infected with the RML strain (ScN2a, Race *et al.*, 1988), N2a#58 cells infected with the 22L strain (L-1, Nishida *et al.*, 2000) and N2a#58 cells infected with the Fukuoka-1 strain (F-3). N2a#58 cells are known to express five times more normal PrP than N2a cells. All cell lines were individually cultured in Opti-MEM (Invitrogen; supplemented with 10% fetal calf serum).

For *in vivo* studies, transgenic mice models Tg7, over-expressing hamster PrP (Race *et al.*, 1995; Priola *et al.*, 2000), and Tga20, expressing five- to eightfold higher levels of murine PrP (Fischer *et al.*, 1996), were used. These models showed substantially shorter incubation periods following intracranial infection with 20 µl of 1% (w/v) 263K scrapie strain homogenate and RML strain, respectively. By 6 weeks post-inoculation, the Tg7 mouse model consistently showed plaque-type PrP deposition in the cerebral white matter between the cortex and hippocampus, and at the disease terminal stage showed synaptic-type deposition in the thalamus, hypothalamus and pons. Similarly, the Tga20 mouse model showed plaque-type deposition in the same brain areas, but not as consistently. Permission for the animal study was obtained from the Animal Experiment Committee of Kyushu University. Each mouse weighed approximately 30 g, and was maintained under deep ether anaesthesia during all surgical procedures.

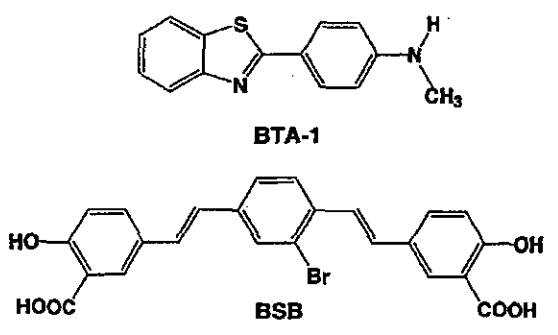


**Fig. 1.** Structures of the chemicals used in this study.

**PrP imaging in pathological sections.** Brain samples of autopsy-diagnosed sporadic CJD cases ($n=3$), GSS cases ($n=2$) and non-TSE control cases with amyloid lesions (Alzheimer's disease, $n=2$) or without them (cerebral infarction, $n=1$; pancreatic cancer, $n=1$) were obtained from the Department of Neuropathology, Kyushu University. Tissue samples of TSE material were immersed in 98% formic acid for 1 h to reduce infectivity. Each tissue sample was embedded in paraffin, and then cut into 7 µm thick sections. Sections of variant CJD brain were kindly provided by James W. Ironside of the CJD Surveillance Unit, Edinburgh, UK. For neuropathological staining, sections were deparaffinized in xylene and hydrated in ethanol. They were then incubated for 30 min in a solution of 1 µM BTA-1 in 50% ethanol, rinsed and examined under a fluorescent microscope (DMRXA, Leica Instruments) with a UV filter set. The sections were washed overnight in 50% ethanol. After verifying clearance of the BTA-1 signal, they were incubated for 30 min in a solution of 1 µM BSB and re-examined under the fluorescent microscope. For comparison, each section was subsequently immunostained as described previously (Doh-ura *et al.*, 2000). Briefly, sections were incubated in 0·3% $H_2O_2$ in absolute methanol for 30 min and then treated by a hydrolytic autoclave procedure (1 mM HCl, 121 °C, 10 min). After rinsing with 50 mM Tris/HCl, pH 7·6, the sections were incubated at 4 °C overnight with a rabbit primary antibody c-PrP, which was raised against a mouse PrP fragment, amino acids 214–228 (1:200; Immuno-Biological Laboratories, Gunma, Japan) (Yokoyama *et al.*, 2001), followed by incubation with a horseradish-peroxidase-conjugated secondary antibody (1:200; Vector Laboratories) at room temperature for 1 h. The coloured reaction product was developed with 3,3'-diaminobenzidine tetrahydrochloride solution. In addition, formalin-fixed brains of diseased Tg7 mice were investigated using the same procedure. To ensure specificity of the anti-PrP antibody, brain sections with other amyloid lesions such as senile plaques were also immunostained. No positive reactions were obtained.

**PrP imaging in presymptomatic mice.** BTA-1 or BSB 10–30 mg (kg body weight)$^{-1}$ in 10% DMSO/saline, or vehicle alone, was administered intravenously into Tg7 mice intracerebrally infected with the 263K strain at 6 weeks post-infection, or into Tga20 mice intracerebrally infected with the RML strain at 8 weeks post-infection. At this point the mice showed no apparent clinical signs of disease. As another control, either chemical was similarly injected into uninfected transgenic mice. The animals were sacrificed at different time-points, and the brains were removed, frozen in powdered dry ice and cut coronally into 10 µm thick sections using a cryostat. The sections were examined under a fluorescent microscope, and then analysed immunohistochemically for PrP as described above.

**$PrP^{Sc}$ inhibition in scrapie-infected cells.** $PrP^{Sc}$ inhibition assays using a cellular model of TSE were performed as described previously (Caughey & Raymond, 1993). Either BTA-1 or BSB in 100% DMSO was added at the designated concentrations to each of the cell lines in 6-well plates when they reached 5% confluency. The final concentration of DMSO in the medium was kept to less than 0·2%. Two controls, one for untreated cells and the other for cells treated with vehicle alone (0·2% DMSO), were prepared. The cultures were allowed to grow to confluence, and then harvested and analysed for $PrP^{Sc}$ content by immunoblotting. Briefly, the cells were lysed with lysis buffer (0·5% sodium deoxycholate, 0·5% Nonidet P-40, PBS) and digested with 20 µg proteinase K ml$^{-1}$ for 30 min at 37 °C. The digestion was terminated with 0·5 mM phenylmethylsulfonyl fluoride, and the samples were centrifuged at 100 000 *g* for 30 min at 4 °C. Pellets were resuspended in 30 µl of sample loading buffer and boiled for 5 min. The samples were separated on a 15%

polyacrylamide Tris/glycine SDS gel and transferred to a PVDF filter (Millipore). $PrP^{Sc}$ was detected using a rabbit polyclonal antibody PrP-2B, which was raised against a mouse/hamster PrP fragment, amino acids 89–103 (1:5000) (Murakami-Kubo *et al.*, 2004), followed by an alkaline phosphatase-conjugated goat anti-rabbit antibody (1:20 000; Promega). Immunoreactive signals were visualized using the CDP-Star detection reagent (Amersham) and analysed densitometrically using image analysis software. More than two independent assays were performed for each experiment.

**Therapeutic treatment in model animals.** BSB dissolved in 10% DMSO/saline at 1 mg per injection was given intravenously to infected Tg7 mice ($n$=5 in each group) or infected Tga20 mice ($n$=7 in each group). The treatment was performed for Tg7 mice at 35 days post-infection (p.i.) and 50 days p.i., and for Tga20 mice at 45 days p.i. and 60 days p.i. Two control groups were prepared for both experimental models: untreated mice and mice treated with vehicle alone. The animals were monitored 5 days a week until the obvious clinical stage was reached, which was the day before or the day of death in Tg7 mice and 4–5 days before death in Tga20 mice. The statistical significance was analysed by one-way ANOVA followed by Scheffé's method for multiple comparisons.

## RESULTS

### Imaging of PrP deposition *in vitro* and *in vivo*

Imaging of PrP deposition in the brain by BTA-1 or BSB was first examined using histopathological specimens from human TSE cases. Both chemicals fluorescently labelled most of the compact PrP plaques in the cerebellar cortices of GSS cases (Fig. 2a and c). No residual fluorescence of BTA-1 was seen after thorough washing (Fig. 2b). The labelling intensity was stronger in the sections labelled with BSB compared with those labelled with BTA-1, but the size of each plaque detected by BTA-1 was on average larger than that detected by BSB. The plaques were counterstained with an antibody against the C terminus of PrP (Fig. 2d). In the sections from a variant CJD case, dense PrP plaques were detectable by both chemicals, whereas most of the immunopositive PrP deposits, such as fine granular deposits and perivacuolar deposits, were not labelled (Fig. 2e–h). In the

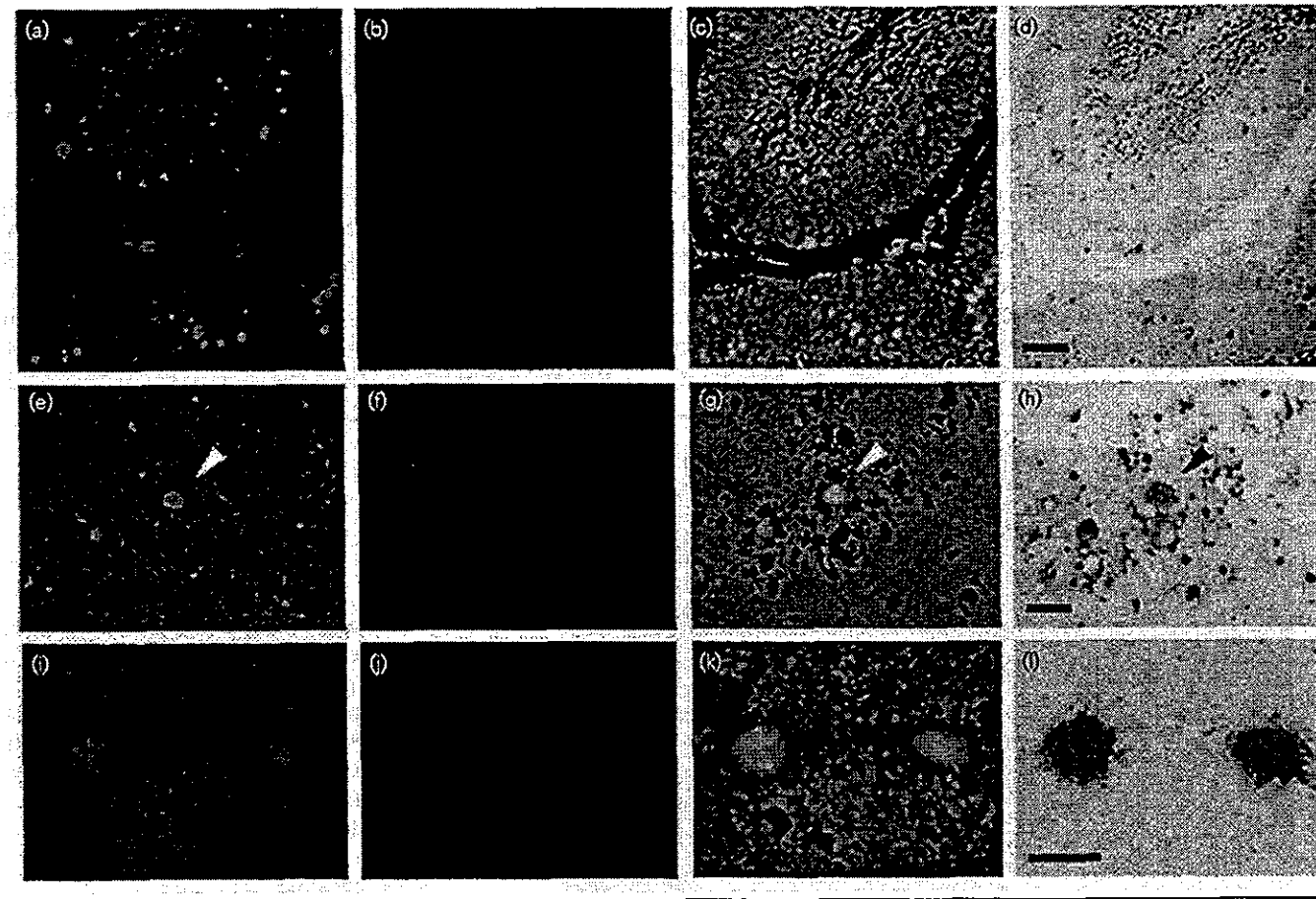


**Fig. 2.** Imaging of PrP aggregates in brains with TSE. PrP plaques were labelled with BTA-1 (a, e and i); no residual signal was seen after washing to remove BTA-1 (b, f and j). The plaques were then labelled with BSB (c, g and k), and subsequently immunostained for PrP (d, h and l). The first row shows a cerebellar section from a GSS case (a–d), the second shows a cerebral cortical section from a variant CJD case (e–h) and the third shows cerebral white matter section from a terminal Tg7 mouse (i–l). Only dense plaques are identified in the variant CJD section; the arrowheads point to the same PrP plaque. In the Tg7 section, PrP plaques in the cerebral white matter between the cortex and hippocampus were labelled. Bars, 100 (a–d) and 50 (e–l) μm.

sections from sporadic CJD cases, neither of the chemicals labelled synaptic-type PrP deposition (data not shown). Non-specific labelling was barely observed after rinsing off the excess chemicals. As reported in previous studies (Mathis *et al.*, 2002; Skovronsky *et al.*, 2000), both chemicals stained senile plaques in Alzheimer's brain, and neither displayed signals in control brain sections without amyloid (data not shown). Similar results to those observed in the human TSE brain sections were obtained from post-mortem brains of Tg7 mice infected with the 263K strain; both chemicals stained the plaque-type PrP deposition in the cerebral white matter between the cortex and hippocampus (Fig. 2i–l). There was no PrP immunohistochemical signal or fluorescent signal in the brains of uninfected Tg7 mice (data not shown).

Since both BTA-1 and BSB have been reported to cross the blood–brain barrier, we performed *in vivo* experiments using Tg7 mice in a later stage of 263K scrapie infection. A bolus injection of BTA-1 labelled PrP plaques in the white matter between the cortex and hippocampus of the affected brains (Fig. 3a and b). Faint cerebrovascular labelling was occasionally observed at 4 h after the injection, but not at 18 h or later. PrP imaging of BSB in the brain *in vivo* was almost as effective as that of BTA-1 (Fig. 3c), but non-specific cerebrovascular labelling was more evident. Images of PrP deposition labelled by BSB were not clearly distinguishable in the cerebrovascular images until 24 h post-administration, but background staining was not seen thereafter. The stability of the signals of PrP deposition was examined at various time-points, and both chemicals remained stably visible at 42 h post-injection. In particular, the BSB labelling signals were relatively stable and visible even at 54 h post-injection. There was no significant labelling after an injection of either chemical to uninfected transgenic mice upon examination after sacrifice 24 h later, or after an injection of vehicle alone to infected mice (data not shown). Similar results were obtained for Tga20 mice infected with the RML strain, although labelled PrP plaques were less frequently observed (data not shown).

## Anti-prion activities *in vitro* and *in vivo*

The anti-prion activities of these chemicals were examined using three cell lines infected with different strains. Both BTA-1 and BSB inhibited $PrP^{Sc}$ formation in ScN2a cells in a dose-dependent manner (Fig. 4a). The concentrations giving 50 % inhibition of $PrP^{Sc}$ formation in ScN2a cells relative to the untreated control ($IC_{50}$) were 4 nM for BTA-1 and 1·4 μM for BSB. However, neither chemical was effective in the other cell lines (Fig. 4b and c). Treatment with vehicle (DMSO) alone showed no significant effects when compared with the untreated control. No apparent cell toxicity of the chemicals was observed up to 10 μM for BTA-1 and 100 μM for BSB. To examine the possibility of interference by the chemicals with immunodetection, BTA-1 or BSB at a concentration 10-fold higher than the $IC_{50}$s were added to lysates of untreated ScN2a cells for 1 h prior to proteinase K digestion. After these treatments, the PrP signals were not affected (data not shown).

Since BSB was potent without significant toxicity at a high concentration of 100 μM in the cell cultures and remained stably bound to PrP aggregates in the affected brains for more than 2 days *in vivo*, we examined whether BSB could be an effective treatment for TSE in two different experimental animal models. As shown in Fig. 5, treatment with BSB at 1 mg prolonged the incubation period of Tga20 mice

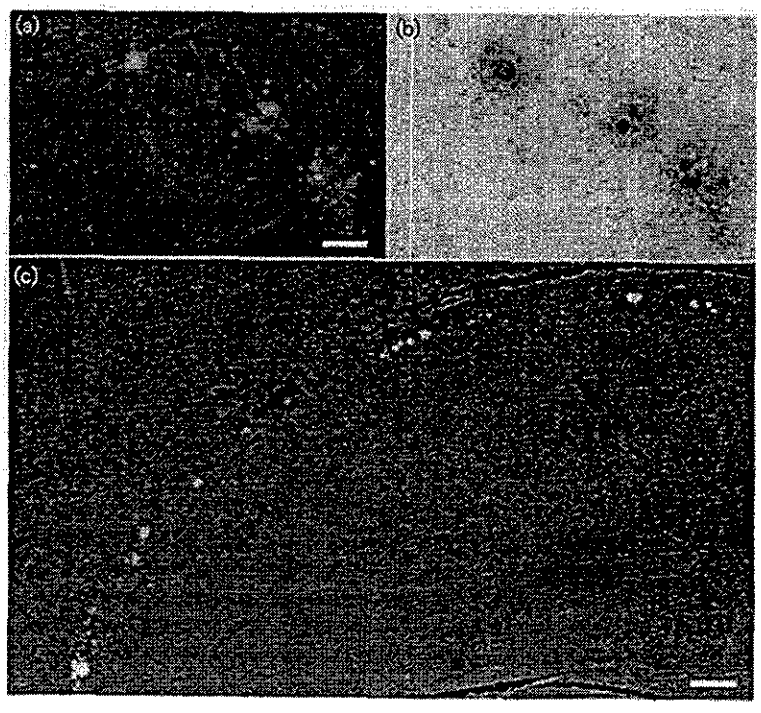


**Fig. 3.** *In vivo* imaging of PrP deposition in the brains of presymptomatic TSE-infected mice. An intravenous bolus injection of BTA-1 was given to Tg7 mice at 6 weeks post-infection, and they were sacrificed 24 h later. PrP plaques in the cerebral white matter between the cortex and hippocampus were detected under a fluorescent microscope (a), and then the brain section was immunostained for PrP (b). Similar results were observed with BSB (c, 24 h post-injection) and immunostaining for PrP (data not shown). Low magnification demonstrates PrP plaques in the cerebral white matter between the cortex and hippocampus were labelled with high specificity. All images are from coronal sections sited around one-third of the distance from the interaural line to the bregma line. Bars, 25 (a, b) and 100 (c) μm.

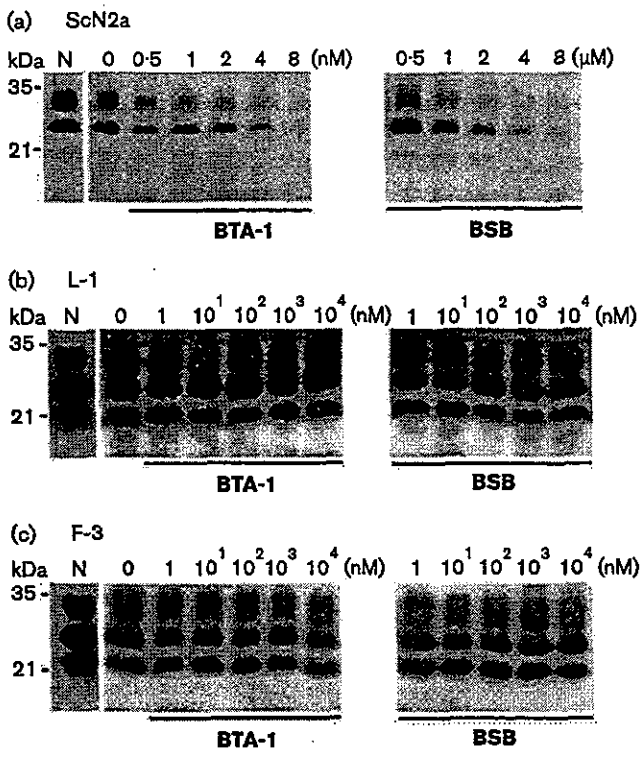


**Fig. 4.** Inhibition of $PrP^{Sc}$ formation in TSE-infected cells by BTA-1 or BSB. Various concentrations of each chemical were added to freshly passaged ScN2a cells in (a), L-1 cells in (b) and F-3 cells in (c), and the $PrP^{Sc}$ levels were analysed by Western blotting. Lanes: N, untreated cells; 0, cells treated with vehicle (DMSO) alone. Bars on the left indicate molecular mass markers at 35 and 21 kDa.

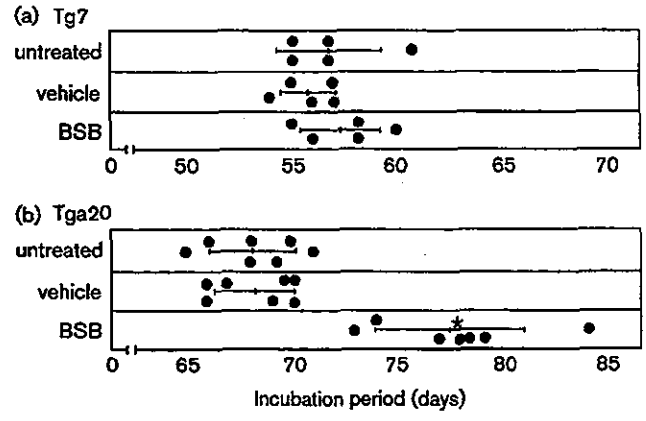


**Fig. 5.** Effects of BSB treatment on TSE-infected mice. BSB was administered to Tg7 mice infected with the 263K strain (a) and Tga20 mice infected with the RML strain (b). The treatment protocol is described in the text. Each closed circle represents an individual animal. Bars represent the mean and standard deviation of the incubation periods of each group. *$P<0.0001$ versus the other groups.

infected with the RML strain by 13·6% (77·6±3·6 days in the BSB-treated group versus 68·3±1·9 days in the vehicle control), whereas no significant prolongation was observed in the same treatment for Tg7 mice infected with the 263K strain (57·4±1·9 days in the BSB-treated group versus 55·8±1·3 days in the vehicle control). The dosage of BSB examined here corresponds to the concentration sufficient to detect PrP plaques *in vivo* as described above, and there were no apparent adverse effects of BSB. No significant differences in incubation times were observed between the untreated controls and the controls treated with vehicle (DMSO) alone (68·1±2·1 days in the untreated control versus 68·3±1·9 days in the vehicle control in Tga20 mice; 57·0±2·4 days in the untreated control versus 55·8±1·3 days in the vehicle control in Tg7 mice).

## DISCUSSION

Both BTA-1 and BSB have been reported to be candidates for PET/SPECT tracers for the evaluation of Alzheimer's disease, and the results of this study have shown that they might also be useful for the evaluation of TSE with certain strains. However, the discrepancy in imaging between the plaque-type and the synaptic-type PrP deposition remains. A previous study demonstrated successful labelling of intracellular A$\beta$(1–42) accumulation in living cells by BSB (Skovronsky *et al.*, 2000), but the same chemical showed no labelling of $PrP^{Sc}$ deposits in ScN2a cells (data not shown). These observations suggest that differences in the structures and/or the microenvironments of these PrP aggregates might account for the discrepancy. Further studies using more sensitive detection methods, such as the use of radiolabelling, might be helpful for evaluation.

Together with previous studies (Mathis *et al.*, 2002; Skovronsky *et al.*, 2000), the current study suggests that both BTA-1 and BSB label various amyloids including A$\beta$ aggregates and PrP aggregates, and are not disease specific. However, these chemicals can be still useful to evaluate amyloid aggregates because anatomical distributions of pathological deposition are quite different between different diseases. For example, A$\beta$ plaques are not, or seldom, observed in the cerebellum, while PrP amyloid plaques are predominantly observed there.

We also demonstrated therapeutic efficacies of these two chemicals. Congo red is well known to inhibit new formation of $PrP^{Sc}$ in ScN2a cells and prolongs the incubation period of infected animals when administered prophylactically (Caughey *et al.*, 1993; Ingrosso *et al.*, 1995). However, Congo red cannot be used as a therapeutic drug because of its inability to cross the blood–brain barrier and its carcinogenicity due to its benzidine structure. BSB, a Congo red analogue, can enter the brain and lacks the benzidine structure. Here BSB showed a low toxicity and was as potent as Congo red in a cellular model, and furthermore, BSB-treatment prolonged the incubation period of the Tga20-RML infected mouse model despite being introduced at a late stage of TSE infection.

There was a discrepancy in the efficacy of BSB between Tg7 mice infected with the 263K strain and Tga20 mice infected with the RML strain. This discrepancy *in vivo* is consistent with that found *in vitro*, since BSB was only effective in ScN2a cells, which are infected with the RML strain. There is a possibility that the differences in susceptibility to these chemicals among the three cell lines might be caused by the differences in the expression levels of normal PrP, because the expression levels of normal PrP in L-1 cells or F-3 cells are five times higher than that of ScN2a cells. However, the data showed that the two chemicals had no effect in either L-1 cells or F-3 cells, even at doses five times greater than the $IC_{50}$ in ScN2a cells. The findings suggest that the therapeutic efficacies of these chemicals are dependent on the TSE strain. In this study, we observed that the chemicals bound tightly to some kinds of PrP aggregates in the pathological sections of TSE, implying that a direct interaction with abnormal PrP molecules may play a role in the inhibition of $PrP^{Sc}$ formation. However, the mechanism of the strain-specific efficacies of these chemicals remains to be elucidated.

Together with previous reports (Caughey *et al.*, 1993; Ingrosso *et al.*, 1995; Supattapone *et al.*, 2002), the current study demonstrated that chemicals with a high affinity for amyloid could be candidates for inhibiting $PrP^{Sc}$ formation and increasing the life-span of TSE-infected animals. We tested this further by examining another chemical, 6-OH-BTA-1, which has recently been reported to facilitate PET studies of Alzheimer's disease (Engler *et al.*, 2002). We observed that this chemical inhibited $PrP^{Sc}$ formation in ScN2a cells with an $IC_{50}$ in the nanomolar order (data not shown), but *in vivo* studies remain to be performed.

In conclusion, BTA-1 and BSB, known as amyloid imaging probes, detected PrP deposition in the TSE brains both *in vitro* and *in vivo* and had anti-prion activities both *in vitro* and *in vivo*, although the efficacy depended upon the strain of TSE. These observations suggest that both could be lead chemicals not only for imaging probes, but also for therapeutic drugs for TSEs caused by certain strains.

## ACKNOWLEDGEMENTS

This study was supported by grants to K. D. from the Ministry of Health, Labour and Welfare (H13-kokoro-025) and the Ministry of Education, Culture, Sports, Science and Technology (13557118, 14021085), Japan. The authors thank Dr James W. Ironside of the CJD Surveillance Unit in Edinburgh University for the variant CJD specimens and Dojindo Laboratories, Kumamoto, Japan, for the BSB compound.

## REFERENCES

**Bacskai, B. J., Klunk, W. E., Mathis, C. A. & Hyman, B. T. (2002).** Imaging amyloid-$\beta$ deposits *in vivo*. *J Cereb Blood Flow Metab* 22, 1035–1041.

**Caughey, B. & Raymond, G. J. (1993).** Sulfated polyanion inhibition of scrapie-associated PrP accumulation in cultured cells. *J Virol* 67, 643–650.

**Caughey, B., Ernst, D. & Race, R. E. (1993).** Congo red inhibition of scrapie agent replication. *J Virol* 67, 6270–6272.

**Demaerel, P., Baert, A. L., Vanopdenbosch, L., Robberecht, W. & Dom, R. (1997).** Diffusion-weighted magnetic resonance imaging in Creutzfeldt–Jakob disease. *Lancet* 349, 847–848.

**Doh-ura, K., Mekada, E., Ogomori, K. & Iwaki, T. (2000).** Enhanced *CD9 expression in the mouse* and human brains infected with transmissible spongiform encephalopathies. *J Neuropathol Exp Neurol* 59, 774–785.

**Engler, H., Nordberg, A., Blomqvist, G. & 11 other authors (2002).** First human study with a benzothiazole amyloid-imaging agent in Alzheimer's disease and control subjects. *Neurobiol Aging* 23, S429.

**Fischer, M., Rulicke, T., Raeber, A., Sailer, A., Moser, M., Oesch, B., Brandner, S., Aguzzi, A. & Weissmann, C. (1996).** Prion protein (PrP) with amino-proximal deletions restoring susceptibility of PrP knockout mice to scrapie. *EMBO J* 15, 1255–1264.

**Hamad, A., Hamad, A., Sokrab, T. E., Momeni, S. & Brown, P. (2001).** Iatrogenic Creutzfeldt–Jakob disease at the millennium. *Neurology* 56, 987.

**Ingrosso, L., Ladogana, A. & Pocchiari, M. (1995).** Congo red prolongs the incubation period in scrapie-infected hamsters. *J Virol* 69, 506–508.

**Mathis, C. A., Bacskai, B. J., Kajdasz, S. T. & 8 other authors (2002).** A lipophilic thioflavin-T derivative for positron emission tomography (PET) imaging of amyloid in brain. *Bioorg Med Chem Lett* 12, 295–298.

**Murakami-Kubo, I., Doh-Ura, K., Ishikawa, K., Kawatake, S., Sasaki, K., Kira, J., Ohta, S. & Iwaki, T. (2004).** Quinoline derivatives are therapeutic candidates for transmissible spongiform encephalopathies. *J Virol* 78, 1281–1288.

**Murata, T., Shiga, Y., Higano, S., Takahashi, S. & Mugikura, S. (2002).** Conspicuity and evolution of lesions in Creutzfeldt–Jakob disease at diffusion-weighted imaging. *Am J Neuroradiol* 23, 1164–1172.

**Nishida, N., Harris, D. A., Vilette, D., Laude, H., Frobert, Y., Grassi, J., Casanova, D., Milhavet, O. & Lehmann, S. (2000).** Successful transmission of three mouse-adapted scrapie strains to murine neuroblastoma cell lines overexpressing wild-type mouse prion protein. *J Virol* 74, 320–325.

**Priola, S. A., Raines, A. & Caughey, W. S. (2000).** Porphyrin and phthalocyanine antiscrapie compounds. *Science* 287, 1503–1506.

**Prusiner, S. B. (1991).** Molecular biology of prion diseases. *Science* 252, 1515–1522.

**Race, R. E., Caughey, B., Graham, K., Ernst, D. & Chesebro, B. (1988).** Analyses of frequency of infection, specific infectivity, and prion protein biosynthesis in scrapie-infected neuroblastoma cell clones. *J Virol* 62, 2845–2849.

**Race, R. E., Priola, S. A., Bessen, R. A., Ernst, D., Dockter, J., Rall, G. F., Mucke, L., Chesebro, B. & Oldstone, M. B. (1995).** Neuron-specific expression of a hamster prion protein minigene in transgenic mice induces susceptibility to hamster scrapie agent. *Neuron* 15, 1183–1191.

**Skovronsky, D. M., Zhang, B., Kung, M. P., Kung, H. F., Trojanowski, J. Q. & Lee, V. M. (2000).** *In vivo* detection of amyloid plaques in a mouse model of Alzheimer's disease. *Proc Natl Acad Sci U S A* 97, 7609–7614.

**Supattapone, S., Nishina, K. & Rees, J. R. (2002).** Pharmacological approaches to prion research. *Biochem Pharmacol* 63, 1383–1388.

**Will, R. G., Ironside, J. W., Zeidler, M. & 7 other authors (1996).** A new variant of Creutzfeldt–Jakob disease in the UK. *Lancet* 347, 921–925.

**Yokoyama, T., Kimura, K. M., Ushiki, Y., Yamada, S., Morooka, A., Nakashiba, T., Sassa, T. & Itohara, S. (2001).** *In vivo* conversion of cellular prion protein to pathogenic isoforms, as monitored by conformation-specific antibodies. *J Biol Chem* 276, 11265–11271.

THE JOURNAL OF BIOLOGICAL CHEMISTRY
Vol. 279, No. 22, Issue of May 28, pp. 23661–23667, 2004
Printed in U.S.A.


# A Pitfall in Diagnosis of Human Prion Diseases Using Detection of Protease-resistant Prion Protein in Urine

## CONTAMINATION WITH BACTERIAL OUTER MEMBRANE PROTEINS*

Received for publication, January 8, 2004, and in revised form, March 12, 2004
Published, JBC Papers in Press, March 18, 2004, DOI 10.1074/jbc.M400187200

**Hisako Furukawa‡§, Katsumi Doh-ura¶, Ryo Okuwaki‖ Susumu Shirabe** Kazuo Yamamoto‖, Heiichiro Udono‡‡, Takashi Ito§§, Shigeru Katamine‖, and Masami Niwa‡**

*From the ‡Departments of Pharmacology 1, ‖Molecular Microbiology and Immunology, the **First Department of Internal Medicine, §§Department of Biochemistry, Nagasaki University Graduate School of Biomedical Sciences, 1-12-4 Sakamoto, Nagasaki 852-8523, Japan, the ¶Department of Prion Research, Tohoku University Graduate School of Medicine, 2-1 Seiryo-cho, Sendai 980-8575, Japan, and the ‡‡Laboratory for Immunochaperones, Research Center for Allergy and Immunology, RIKEN Yokohama Institute, Tsurumi, Yokohama 230-0045, Japan*

**Because a definite diagnosis of prion diseases relies on the detection of the abnormal isoform of prion protein ($PrP^{Sc}$), it has been urgently necessary to establish a non-invasive diagnostic test to detect $PrP^{Sc}$ in human prion diseases. To evaluate diagnostic usefulness and reliability of the detection of protease-resistant prion protein in urine, we extensively analyzed proteinase K (PK)-resistant proteins in patients affected with prion diseases and control subjects by Western blot, a coupled liquid chromatography and mass spectrometry analysis, and N-terminal sequence analysis. The PK-resistant signal migrating around 32 kDa previously reported by Shaked *et al.* (Shaked, G. M., Shaked, Y., Kariv-Inbal, Z., Halimi, M., Avraham, I., and Gabizon, R. (2001) *J. Biol. Chem.* 276, 31479–31482) was not observed in this study. Instead, discrete protein bands with an apparent molecular mass of ~37 kDa were detected in the urine of many patients affected with prion diseases and two diseased controls. Although these proteins also gave strong signals in the Western blot using a variety of anti-PrP antibodies as a primary antibody, we found that the signals were still detectable by incubation of secondary antibodies alone, *i.e.* in the absence of the primary anti-PrP antibodies. Mass spectrometry and N-terminal protein sequencing analysis revealed that the majority of the PK-resistant 37-kDa proteins in the urine of patients were outer membrane proteins (OMPs) of the *Enterobacterial* species. OMPs isolated from these bacteria were resistant to PK and the PK-resistant OMPs from the *Enterobacterial* species migrated around 37 kDa on SDS-PAGE. Furthermore, nonspecific binding of OMPs to antibodies could be mistaken for $PrP^{Sc}$. These findings caution that bacterial contamination can affect the immunological detection of prion protein. Therefore, the presence of *Enterobacterial* species should be excluded in the immunological tests for $PrP^{Sc}$ in clinical samples, in particular, urine.**

Prion diseases are a group of neurodegenerative disorders pathologically characterized by accumulation of an abnormal isoform of prion protein ($PrP^{Sc}$) in the central nervous system. A definite diagnosis of prion diseases relies on the detection of $PrP^{Sc}$ (1). Concerning the link between bovine spongiform encephalopathy and variant Creutzfeldt-Jakob disease (CJD),[1] the iatrogenic occurrence of prion diseases after dural transplantation, and the recent remarkable progress in therapeutic approaches have made it urgently necessary to establish a non-invasive *in vivo* test to enable a definite diagnosis of human prion diseases in the early or preclinical stage of the disease.

Diffusion-weighted magnetic resonance imaging of the brain is currently one of the most helpful techniques to detect abnormal high intensity lesions in the cerebral cortices and basal ganglia in the early stage of the disease (2). The detection of 14-3-3 proteins and measurement of phosphorylated tau protein in the cerebrospinal fluid has been found to be useful in supporting the clinical diagnosis of CJD (3,4). Although these tests are clinically useful, they are surrogate markers and therefore cannot provide direct evidence of the presence of $PrP^{Sc}$. Moreover, although a brain biopsy can reveal the deposition of $PrP^{Sc}$ in the brain (5), it is highly invasive and is not suitable for preclinical screening or early diagnosis. Detection of $PrP^{Sc}$ in body fluids such as blood and cerebrospinal fluid has been extensively investigated, but these tests still need a new technological device to increase the sensitivity (6).

As a potentially non-invasive diagnostic test, Shaked *et al.* (7) reported the presence of protease-resistant PrP in the urine ($UPrP^{Sc}$) of humans and animals affected with prion diseases. Their data suggests that $UPrP^{Sc}$ will reflect the presence of $PrP^{Sc}$ in the central nervous system and will also be a useful preclinical diagnostic test for prion diseases. In the present study, we have examined the urine protein of humans affected with prion diseases and controls using Western blot analysis to evaluate diagnostic usefulness and reliability of the $UPrP^{Sc}$ assay in human prion diseases. A detailed analysis using coupled liquid chromatography and mass spectrometry (LC/MS) and N-terminal protein sequencing revealed that bacterial contamination might account for the misinterpretation in the interpretation of protease-resistant protein in urine.

* This work was supported by grants from the Ministry of Health, Labor and Welfare, Japan and the Kurozumi Medical Foundation, Japan (to H. F.). The costs of publication of this article were defrayed in part by the payment of page charges. This article must therefore be hereby marked "*advertisement*" in accordance with 18 U.S.C. Section 1734 solely to indicate this fact.

§ To whom correspondence should be addressed: Dept. of Pharmacology 1, Nagasaki University Graduate School of Biomedical Sciences, 1-12-4 Sakamoto, Nagasaki 852-8523, Japan. Tel.: 81-95-849-7043; Fax: 81-95-849-7044; E-mail: hisako@net.nagasaki-u.ac.jp.

[1] The abbreviations used are: CJD, Creutzfeldt-Jakob disease; PBS, phosphate-buffered saline; PK, proteinase K; OMP, outer membrane proteins.

TABLE I

*Protease-resistant protein in urine and characteristics of patients and controls*

The abbreviations used are: GSS; Garstmann-Sträussler-Scheinker syndrome; HDS-R; revised Hasegawa Dementia Rating Scale; MMSE; Mini-Mental State Examination; and MELAS; mitochondrial myopathy, lactic acidosis, and stroke-like episodes.

| Clinical diagnosis[a] | No. of cases | Mean age[b] | Mean clinical duration at examination | CSF 14–3-3 protein positive ratio | Brain DWI MRI[c] positive ratio | Protease-resistant protein in urine[d] positive ratio |
|---|---|---|---|---|---|---|
| | | *years* | *months* | | % | |
| Prion diseases | | | | | | |
| Sporadic CJD | 45 | 65.9 (42-83) | 5.5 (1.5-18) | 93.5 (29/31) | 75.0 (15/20) | 66.7 (30/45) |
| Dural graft-associated CJD | 4 | 53.8 (15-69) | 20.5 (6-48) | 100 (3/3) | 25.0 (1/4) | 100 (4/4) |
| Familial CJD (E200K) | 2 | 58.5 (53-64) | 3.8 (3.5-4) | 50 (1/2) | 100 (2/2) | 100 (2/2) |
| GSS (P102L) | 3 | 57.3 (47-72) | 45.3 (28-72) | NE[e] | NE | 66.7 (2/3) |
| | 54 | 58.9 | 9.58 | 91.7 (33/36) | 69.2 (18/26) | 70.4 (38/54) |

| | | | | Mean scores | | |
|---|---|---|---|---|---|---|
| | | | | HDS-R | MMSE | |
| Diseased controls with dimentia | | | | | | |
| Alzheimer's disease | 19 | 74.2 (56-87) | NA[f] | 13.5 (0-23) | 18.8 (0-30) | 0 (0/19) |
| Cerebrovascular dementia | 1 | 76 | NA | 19 | 24 | 0 (0/1) |
| Diseased controls without dimentia | | | | | | |
| Diabetes mellitus | 7[g] | 67.5 (53-75) | NA | NE | NE | 14.3 (1/7)[h] |
| Cerebral infarction | 6[g] | 73.3 (62-77) | NA | NE | NE | 16.7 (1/7)[h] |
| Multiple sclerosis | 4 | 49.3 (24-62) | NA | NE | NE | 25.0 (1/4) |
| Pneumonia | 2 | 72.0 (70-74) | NA | NE | NE | 0 (0/2) |
| Epilepsy | 2 | 46.0 (20-72) | NA | NE | NE | 0 (0/2) |
| Myasthenia gravis | 1 | 35 | NA | NE | NE | 0 (0/1) |
| Encephalitis | 1 | 57 | NA | NE | NE | 0 (0/1) |
| Chronic renal failure | 1 | 79 | NA | NE | NE | 0 (0/1) |
| MELAS | 1 | 21 | NA | NE | NE | 0 (0/1) |
| | 23 | 27.5 (19-59) | | NE | NE | 0 (0/23) |
| Healthy controls | | 56.5 | | | | 3 (2/66) |

[a] Clinical diagnosis of prion diseases was performed in accordance with the criteria proposed by WHO.
[b] Mean age at onset in groups of prion diseases, at examination in controls.
[c] Abnormal high intensity signals in cerebral cortices or basal ganglia on diffusion-weighted (DWI) MRI of the brain.
[d] Determined by the presence of PK-resistant signal around 37 kDa.
[e] NE, not examined.
[f] NA, data not available.
[g] Two patients were included in both groups.
[h] Identical patient.

## EXPERIMENTAL PROCEDURES

*Analysis of Human Urine—Urine samples were collected from patients affected with prion diseases and control subjects under informed consent (Table I). A clinical diagnosis of prion disease was made by neurologists in order to follow the diagnostic criteria proposed by the World Health Organization (1). First morning urine samples were used whenever possible.*

Protein was isolated from urine as previously described by Shaked *et al.* (7) with minor modifications. After dialysis and sedimentation by ultracentrifugation, the pellets obtained from 15 ml of urine were re-suspended in 30 μl of PBS (pH 7.4) containing 0.5% Nonidet P-40 and 0.5% sodium deoxycholate, instead of STE buffer containing 2% Sarkosyl, and digested with 40 μg/ml proteinase K (PK) (Roche Diagnostics) at 37 °C for 1 h. In several samples, urine protein was re-suspended in 2% Sarkosyl STE buffer prior to PK digestion as described by Shaked *et al.* (7). Western blot analysis was performed using monoclonal antibodies 3F4 at 1:10,000 (Signet Laboratories), 6H4 at 1:5,000 (Prionics, Switzerland), or 3O8 at 1:1,000 (Cayman Chemical) followed by incubation with donkey-derived anti-mouse IgG (AP192A, Chemicon), goat-derived anti-mouse IgG (H + L) (S372B, Promega), or the $F(ab')_2$ fragment of rabbit-derived anti-mouse IgG (710–4520, Rockland) and development in a chemiluminescent substrate (*CDP Star* or *ECL-Plus*, Amersham Biosciences). Some blots were labeled with PrP2B, rabbit-derived polyclonal antibody raised against PrP89-103, followed by incubation with donkey-derived anti-rabbit IgG (AP182A, Chemicon). In some blots, incubation with primary antibody was omitted for the experimental purpose.

*Coupled Liquid Chromatography and Mass Spectrometry (LC/MS) Analysis of Protease-resistant Proteins*—A PK-resistant signal of 37 kDa on a SDS-polyacrylamide gel was cut out and transferred to a clean, siliconized Eppendorf tube. In-gel digestion was performed as previously described (8). After an overnight incubation of gels with trypsin at 37 °C, the digested protein was extracted twice with 50% acetonitrile, 50% trifluoroacetic acid and concentrated by vacuum centrifugation. An LC/MS analysis was performed using the QSTAR XL system (Applied Biosystems) and MAGIC 2002 liquid chromatography (Michrom BioResourse). The obtained protein masses were queried against entries for all species in the SwissProt data base using the Mascot Search program offered by Matrix Science.[2]

*N-terminal Protein Sequencing*—PK-resistant protein was obtained from the urine of patients sCJD 4, 5, and 7 and dural graft-associated CJD-1 as described above, or from urine of other patients as described by Shaked *et al.* (7). After separation of the protein samples by 12% mini SDS-PAGE gels (Bio-Rad), proteins were transferred onto Immobilon-P$^{SQ}$ transfer membrane (Millipore). PK-resistant bands visualized by Coomassie Brilliant Blue staining were cut out and stored at 4 °C until the sequencing procedure. N-terminal protein sequencing by automated Edman degradation was performed using the Procise 491cLC protein sequencer (Applied Biosystems), as previously described (9). N-terminal sequencing proceeded for 13 to 23 cycles. The obtained amino acid sequences were queried against entries for all species in the SwissProt data base using the FASTA search program offered by GenomeNet.[3]

*Assays of Protease Resistance of Outer Membrane Proteins (OMP)*—OMPs were isolated from *Klebsiella pneumoniae* and *Salmonella typhimurium* as previously described (10) with minor modifications. In brief, cells harvested from overnight cultures in Super Broth medium were recovered by centrifugation. After washing with 10 mM Tris-HCl (pH 7.2), 5 mM $MgCl_2$, cells were broken by sonication. Unbroken cells were eliminated and cell envelopes were recovered at 100,000 × *g* for 1 h. After solubilization in 10 mM Tris-HCl (pH 7.2), 5 mM $MgCl_2$, 0.5% Nonidet P-40, 0.5% deoxycholate for 30 min at 25 °C, insoluble OMPs were recovered by ultracentrifugation at 100,000 × *g* for 1 h. OMPs were resuspended in 0.5% Nonidet P-40, 0.5% deoxycholate in PBS (pH 7.4), or 2% Sarkosyl STE buffer and digested with 40 μg/ml of PK at 37 °C for 1 h, under the same conditions as urine proteins. In parallel, 15 μg of ovalbumin was digested with PK as a control.

*Binding of OMPs to $F(ab')_2$ Fragment of Immunoglobulin*—Isolated OMPs were separated by 12% SDS-PAGE and transferred onto the

[2] Available at www.matrixscience.com.
[3] fasta.genome.ad.jp.

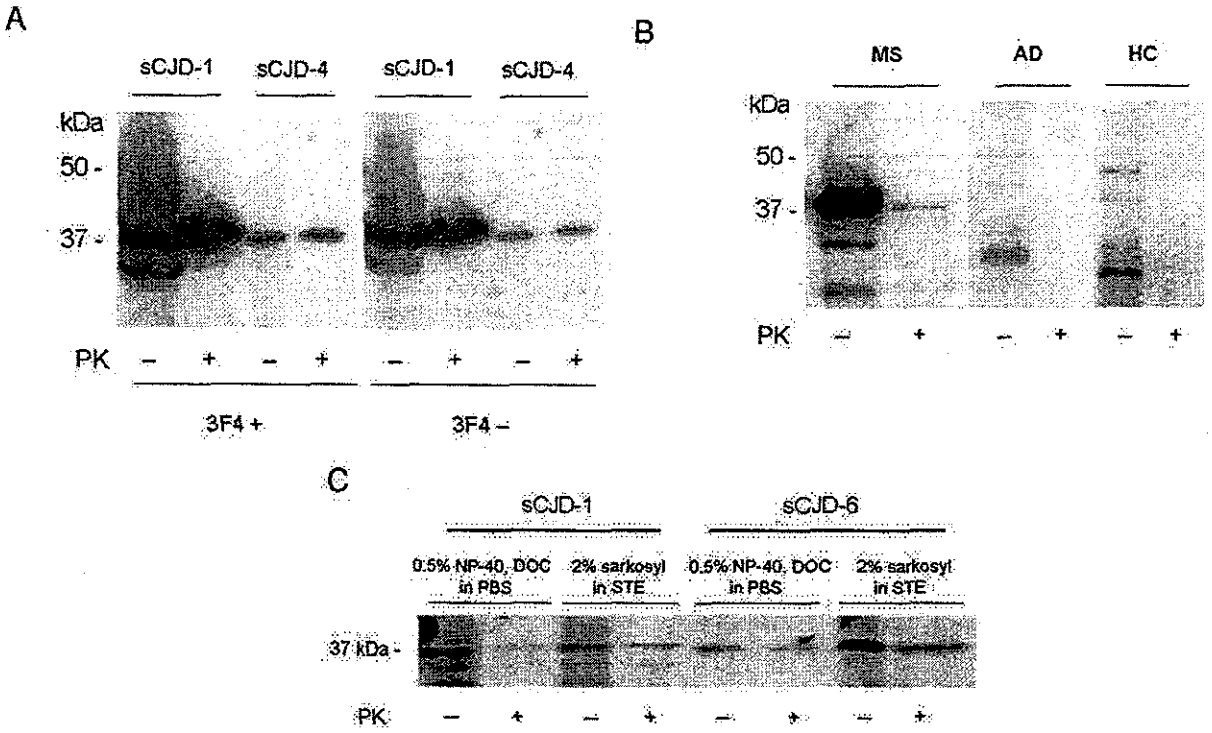


FIG. 1. **Western blot analysis of urine proteins.** Protein obtained from 15 ml (*A* and *B*) or 7.5 ml (*C*) of urine was applied in each lane. *PK*, digestion with proteinase K. *A*, urine proteins were drawn from sCJD-1 and sCJD-4 patients. Patient ID number corresponds to that in Table III. Proteins were re-suspended in PBS (pH 7.4) containing 0.5% Nonidet P-40 and 0.5% deoxycholate (*DOC*). The blot was probed with 3F4 monoclonal antibody followed by incubation with secondary antibody AP192A (*left panel*) or incubated with secondary antibody omitting the probing with 3F4 (*right panel*). *B*, urine proteins were obtained from patients with multiple sclerosis (*MS*) bearing a urethral catheter, with Alzheimer's disease (*AD*), and from a healthy control subject (*HC*). Proteins were re-suspended in PBS (pH 7.4) containing 0.5% Nonidet P-40 and 0.5% deoxycholate. A PK-resistant signal was detected in one patient affected with MS. The membranes were probed with 3F4 monoclonal antibody followed by incubation with AP192A. *C*, urine proteins were drawn from sCJD-1 and sCJD-6 patients, and re-suspended in PBS (pH 7.4) containing 0.5% Nonidet P-40 and 0.5% deoxycholate or in STE buffer containing 2% Sarkosyl as described by Shaked *et al.* (7). The blot was incubated with a rabbit-derived $F(ab')_2$ fragment of anti-mouse IgG.

polyvinylidene difluoride membrane. To determine whether OMPs bind to antibodies via the Fc region of immunoglobulin, the membrane was incubated with the $F(ab')_2$ fragment of anti-mouse IgG conjugated with alkaline phosphatase (710–4520, Rockland) after blocking with 5% nonfat milk. The membrane was then developed in a chemiluminescent substrate (CDP Star, Amersham Biosciences).

## RESULTS

*PK-resistant Protein in the Urine of Humans Affected with Prion Diseases Directly Reacted with Secondary Antibodies*—The results of urine protein examination and patient and control characteristics are summarized in Table I. We examined the PK sensitivity of urine proteins of patients affected with prion diseases ($n = 54$), healthy controls ($n = 23$), and disease control patients with ($n = 20$) and without dementia ($n = 23$). Clinical durations between disease onset and urine collection were 1.5 to 72 months in prion diseases. 14-3-3 protein in cerebrospinal fluid was frequently positive in sporadic CJD (93.5%, 29/31) and dural graft-associated CJD (100%, 3/3). Abnormal high intensity signals in the cerebral cortices or basal ganglia were observed in the majority of patients with sporadic CJD (75.0%, 15/20). Most patients carried methionine homozygosity at codon 129 in the prion protein gene (PRNP), except for one case that was affected with Gerstmann-Sträussler-Scheinker syndrome. No patients carried lysine polymorphisms at codon 219 in the PRNP.

Three kinds of signals migrating around 37, 28, and 22 kDa were observed after PK treatment of the urine. PK-resistant signals of 37 kDa were prominent and observed in all positive cases, whereas the other two signals were usually faint and not always observed in all the positive cases. The signals of 28 kDa were also observed in controls after digestion with PK, suggesting that it represented a nonspecific signal because of PK itself. PK-resistant signals around 32 kDa, detected by Shaked *et al.* (7) in CJD patients, were not observed in the present study. Therefore, we decided to utilize the 37-kDa signal as a PK-resistant protein in urine in this study. PK-resistant protein signals of 37 kDa were detectable in 70.4% (38/54) of the patients affected with prion diseases, whereas 3% (2/66) of the control subjects were positive for PK-resistant signals. The PK-resistant signal was not detectable in healthy controls or diseased controls with dementia (Table I and Fig. 1*B*).

Although PK-sensitive and -resistant signals were detectable by labeling with 3F4 (Fig. 1*A*, *left panel*), 6H4, 3O8, or PrP2B (data not shown), these signals were also detectable with anti-mouse IgG antibody alone, omitting the incubation with 3F4 (Fig. 1*A*, *right panel*). This phenomenon was observed in all cases (11 cases; sporadic CJD, one case; dura-associated CJD) tested and reproducible using three kinds of anti-mouse IgG antibodies (AP192A, Chemicon; S372B, Promega; and 710–4520, Rockland) and an anti-rabbit IgG antibody (AP182A, Chemicon) (data not shown).

To examine the possible influence of assay conditions on the detection of PK-sensitive or -resistant signals, urine proteins were re-suspended prior to PK digestion in 2% Sarkosyl STE buffer as described previously by Shaked *et al.* (7) or in 0.5% Nonidet P-40, 0.5% deoxycholate, PBS buffer. As shown in Fig. 1*C*, 37-kDa signals were similarly detectable in both assay conditions, indicating that the difference of the assay conditions did not influence the detection of these signals.

*Contamination of Urine with Bacterial Outer Membrane Proteins*—To characterize the PK-resistant protein of 37 kDa on Western blot analysis, the bands from the urine of three pa-

TABLE II
*List of proteins detected by LC/MS analysis*
Protein masses were queried against entries for all species in the SwissProt database. Patient's ID correspond to that in Table III.

| Patient ID | Significant hits | | Peptides matched |
|---|---|---|---|
| | *Protein identification* | *Species* | |
| sCJD-1[a] | Outer membrane protein C precursor | *K. pneumoniae* | 11 |
| | Outer membrane protein C, chain A | *K. pneumoniae* | 8 |
| | Outer membrane protein C precursor | *S. typhimurium* | 3 |
| sCJD-2 | Outer membrane protein C precursor | *E. coli* | 13 |
| | Outer membrane protein C precursor | *E. coli* O157:H7 | 13 |
| | Outer membrane protein C precursor | *S. typhimurium* | 4 |
| | Translation initiation factor IF-2 | *Geobacillus stearothermophilus* | 3 |
| | Outer membrane protein S2 precursor | *S. typhimurium* | 2 |
| | Outer membrane protein F precursor | *S. typhimurium* | 2 |
| sCJD-3 | Outer membrane protein C precursor | *E. coli* O157:H7 | 16 |
| | Outer membrane protein C precursor | *E. coli* O6 | 11 |
| | Outer membrane protein C precursor | *S. typhimurium* | 5 |
| | Outer membrane protein C precursor | *K. pneumoniae* | 4 |
| | Outer membrane protein (fragment) | *Sodalis glossinidius* | 2 |
| | Outer membrane protein S1 precursor | *S. typhimurium* | 2 |
| | Outer membrane protein S2 precursor | *S. typhimurium* | 2 |
| | Outer membrane protein F precursor | *S. typhimurium* | 2 |
| | Glial fibrillary acidic protein homolog | *Carassius auratus* | 2 |
| | Elongation factor P-like protein | *S. typhimurium* | 1 |

[a] sCJD, sporadic CJD.

tients were purified from the SDS-polyacrylamide gel and prepared for LC/MS as previously described (8). One of these patients was diagnosed as probable sporadic CJD and the others were pathologically definite sporadic CJD. Protein mass analysis using LC/MS demonstrated that the major component of the PK-resistant signal was the OMPs of bacteria such as *Escherichia coli, K. pneumoniae,* and *S. typhimurium* (Table II). No molecules of human origin, including PrP and immunoglobulin, were detected with any significance. Fig. 2 demonstrated the results of LC/MS analysis of a patient (sCJD-2).

We performed an N-terminal sequencing analysis to confirm the results of the LC/MS more quantitatively. It revealed that prominent PK-resistant signals in the urine of these three patients and all other patients examined (10/10) consisted of a mature chain of OMPs (Table III). Neither PrPs nor immunoglobulins were detected.

As described above, two other minor signals migrating around 28 and 22 kDa were observed on SDS-PAGE after PK treatment in the urine of some patients and controls. The N-terminal protein sequence analysis revealed that the signal at 28 kDa corresponded to the fragment of PK used for the assay and another signal at 22 kDa corresponded to the fragment of OMPs.

*OMPs Are Resistant to PK*—To evaluate PK sensitivity, OMPs were isolated from overnight cultured *K. pneumoniae* or *S. typhimurium* in Super Broth medium. After digestion with PK, a considerable amount of OMPs remained undigested and migrated around 37 kDa on SDS-PAGE (Fig. 3*A*, *fourth* and *sixth lanes*), whereas ovalbumin was completely digested under the same conditions (Fig. 3*A*, *second lane*). The electrophoretic mobility of PK-resistant OMPs was similar to that of the PK-resistant urine protein isolated from a patient affected with sporadic CJD (Fig. 3*A*, *seventh lane*).

*OMPs Reacted with the F(ab') Portion of Immunoglobulins*—To evaluate if OMPs bind to the Fc region of immunoglobulins like protein A, a cell wall component of *Staphylococcus aureus*, one of the gels was blotted onto a polyvinylidene difluoride membrane to perform Western blot analysis. As shown in Fig. 3*B*, OMPs bound to the $F(ab')_2$ fragment of anti-mouse IgG, indicating that OMPs bind to immunoglobulins in a manner that is different from that of protein A with immunoglobulins. This observation as well as PK resistance of OMPs was not influenced by the difference in assay conditions (Fig. 3*C*).

## DISCUSSION

In the present study, we found that the PK-resistant protein was frequently detected in the urine of patients affected with prion diseases. However, the LC/MS and N-terminal protein sequencing analysis revealed that the majority of PK-resistant proteins in the urine of patients, which migrated around 37 kDa on SDS-PAGE and reacted non-specifically with several secondary antibodies, comprised OMPs of bacteria such as *E. coli, K. pneumoniae,* and *S. typhimurium,* the popular causative agents for urinary tract infections. This finding indicated that bacterial contamination of urine might cause false-positive results in the assay for detecting $UPrP^{Sc}$.

It is known that urinary tract infections associated with urethral catheterization is the most common nosocomial infection and is often asymptomatic. In this study, the majority of patients affected with prion diseases were already bearing catheters because of severe deterioration of intellectual and motor functions as they were suspected to be suffering from prion diseases. Furthermore, two of the diseased control patients with positive PK-resistant urine protein were also bearing persistent or intermittent urethral catheters. One patient suffered from neurogenic bladder because of multiple sclerosis and another was long bedridden because of cerebral infarction. The signal intensity decreased after PK digestion in a patient affected with multiple sclerosis (Fig. 1*B*), whereas it was not significant in patients affected with sporadic CJD (Fig. 1*A*). Differences in bacterial species or growth conditions in urine between the cases might cause such a variation in PK sensitivity of OMPs. On the other hand, all diseased controls affected with Alzheimer's disease or cerebrovascular dementia were outpatients; therefore, they were thought to be at lower risk of urinary tract infections. These circumstances strongly supported that possible bacterial contamination resulted in the detection of confusing PK-resistant protein in urine.

OMPs are 36- to 39-kDa membrane spanning proteins that form channels in the outer membranes of Gram-negative bacteria. The primary and secondary structures of OMPs are well conserved in *Enterobacterial* species containing 16-stranded antiparallel $\beta$ barrels to form channels (11). Biochemically,

A

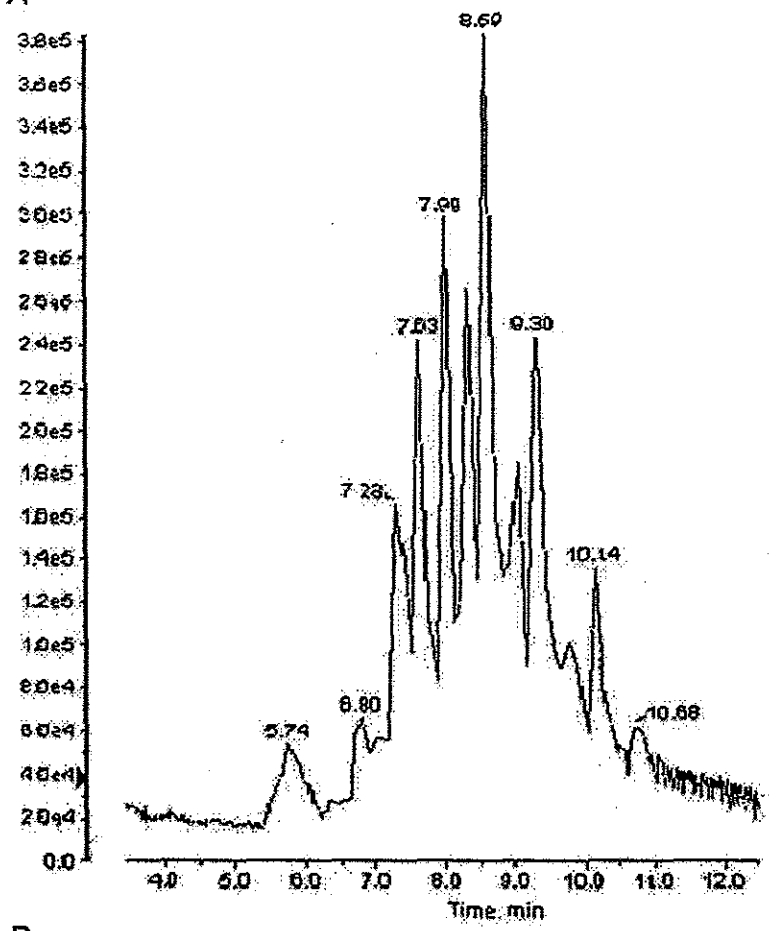


B

| R.Time | Ion observed | Mr(expt) | Mr(calc) | Delta | Miss | Peptide |
|---|---|---|---|---|---|---|
| 5.39 | 470.27 | 938.53 | 938.47 | 0.06 | 0 | AETYTGGLK |
| 5.56 | 586.27 | 1170.52 | 1170.50 | 0.03 | 0 | SVDGDQTYMR |
| 5.90 | 568.77 | 1135.53 | 1135.49 | 0.04 | 0 | NMSTYVDYK + Oxidation (M) |
| 6.80 | 443.72 | 885.42 | 884.41 | 1.00 | 0 | GNGFATYR |
| 7.26 | 607.65 | 1819.91 | 1819.84 | 0.07 | 1 | RTDDQNSPLYIGNGDR |
| 7.28 | 560.76 | 1119.51 | 1119.49 | 0.02 | 0 | NMSTYVDYK |
| 7.63 | 432.55 | 1294.62 | 1294.58 | 0.04 | 0 | VDGLHYFSDDK |
| 7.99 | 645.79 | 1289.56 | 1289.57 | -0.00 | 0 | FQDVGSFDYGR |
| 8.11 | 862.76 | 2585.27 | 2584.20 | 1.06 | 1 | TDDQNSPLYIGNGDRAETYTGGLK |
| 8.35 | 720.33 | 1438.66 | 1438.68 | -0.02 | 0 | YVDVGATYYFNK |
| 8.59 | 785.38 | 2353.12 | 2353.10 | 0.02 | 0 | YDANNIYLAAQYTQTYNATR |
| 10.14 | 1117.07 | 2232.12 | 2232.09 | 0.04 | 0 | NTDFFGLVDGLNFAVQYQGK |

C

1 MKVKVLSLLV PALLVAGAAN AAEVYNKDGN KLDLYGKVDG LHYFSDDKSV

51 DGDQTYMRLG FKGETQVTDQ LTGYGQWEYQ TQGNSAENEH NSHTRVAFAG

101 LKFQDVGSFD YGRNYGVVYD VTSWTDVLPE FGGDTYGSDN FMQQRGNGFA

151 TYRNTDFFGL VDGLNFAVQY QGKNGSVSGS GMTNNGEEAL RQNGDGVGGS

201 ITYDYEGFGI GAAVSSSKRT DDQNSPLYIG NGDRAETYTG GLKYDANNIY

251 LAAQYTQTYN ATRVGSLGWA NKAQNFEAVA QYQFDFGLRP SLAYLQSKGK

301 NLGVINGRNY DDEDILKYVD VGATYYFNKN MSTYVDYKIN LLDDNQFTRD

FIG. 2. **LC/MS analysis of the PK-resistant protein in the urine.** Peptides from tryptic digestion of the PK-resistant protein in the urine of sCJD-3 were separated using MAGIC 2002 liquid chromatography and the elute were analyzed by MS. *A*, base peak mass chromatogram of the 37-kDa protein, each peak is labeled with the retention time. *B*, molecular mass and amino acid sequence of each peak originating from the 37-kDa protein. All the determined amino acid sequences were identical to that of OMP of *E. coli* (OmpC precursor) based on the results of the data base search. *R. Time*, retention time; *Mr(expt)*, molecular weight in the experiment; *Mr(calc)*, molecular weight in calculation. *C*, amino acid sequence of OmpC of *E. coli* was shown. *Bold style letters* indicate sequences covered by the results of the LC/MS analysis. The sequence identified by N-terminal sequencing analysis is shown with an *underline*.

TABLE III

*Results of the N-terminal sequence of PK-resistant signal in patients' urine*

Amino acid sequences were queried against entries for all species in the SwissProt database using the FASTA search programs offered by GenomeNet. PK-resistant protein bands with molecular mass about 37 kDa were subjected to the analysis.

| Patient ID | N-terminal sequence | Protein identification and species |
|---|---|---|
| Sporadic *CJD* | | |
| sCJD-1[a] | AEIYNKDGNK | OmpC, *K. pneumoniae* |
| sCJD-2[a] | AEVYNKDGNK | OmpC, *E. coli* |
| sCJD-3[a] | AEVYNKDGNK | OmpC, *E. coli* |
| sCJD-4 | AEVYNKJDGNKLDLYGKVDGL | OmpC, *E. coli* |
| sCJD-5 | AEIYNKDGNKLDLYG | OmpC, *K. pneumoniae*, or OmpF, *S. typhimurium* |
| sCJD-6[a] | AEVYNKDGNKLDLYG | OmpC, *E. coli* |
| sCJD-7 | AEVLNKDONK | OmpC, *E. coli* |
| sCJD-8[a] | AEVYNKDGNKL | OmpC, *E. coli* |
| sCJD-9[a] | AEVYDKDGKNLDL | Omp *Sodalis glossinidius* |
| sCJD-10[a] | AEVYNKDGNKL | OmpC, *E. coli* |
| sCJD-11[a] | AEVYNKDGNKLDLYG | OmpC, *E. coli* |
| Dural graft-associated CJD | | |
| 1 | AEVYNKDGNKLDLYG | OmpC, *E. coli* |
| 2[a] | AEIYNKDGNKLDLYG | OmpC *K. pneumoniae*, or OmpF, *S. typhimurium* |

[a] Urine samples were re-suspended in STE buffer containing 2% Sarkosyl as described by Shaked *et al.* (7) or otherwise in PBS containing 0.5% Nonidet P-40 and 0.5% deoxyehdate.

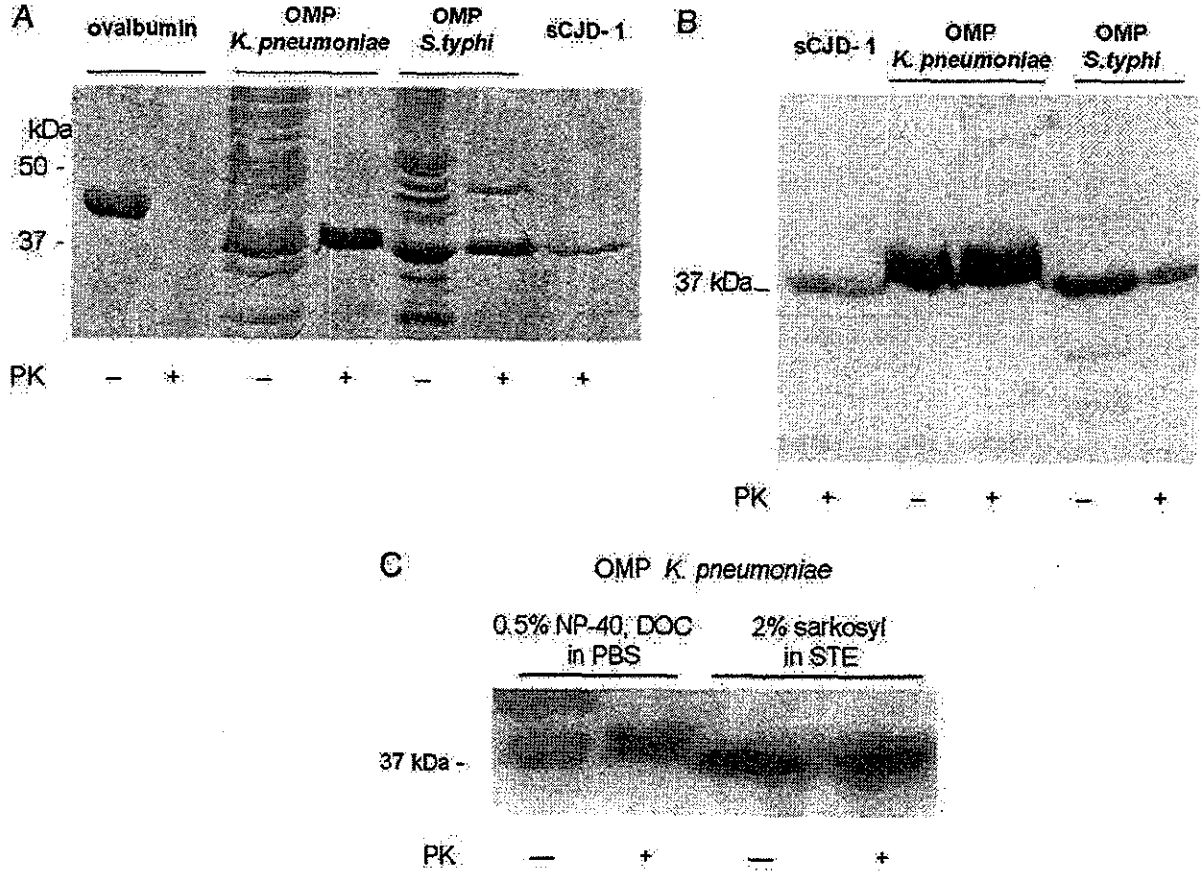


FIG. 3. **PK sensitivity and immunoreactivity of OMPs of *K. pneumoniae* and *S. typhimurium*.** *A*, OMPs isolated from *K. pneumoniae* and *S. typhimurium*, and protein isolated from 15 ml of urine of sCJD-1 patient were digested with PK. Proteins were re-suspended in PBS (pH 7.4) containing 0.5% Nonidet P-40 and 0.5% deoxycholate (*DOC*). An OMP homogenate containing 30 μg of protein was applied in each lane. Fifteen micrograms of ovalbumin was used as a control. After the electrophoretic separation, the polyacrylamide gel was stained with Coomassie Brilliant Blue. *B*, after separation by SDS-PAGE, the gel was blotted onto a polyvinylidene difluoride membrane. Rabbit-derived $F(ab')_2$ fragment of anti-mouse IgG was used as a probe. *C*, OMPs isolated from *K. pneumoniae* were re-suspended in PBS (pH 7.4) containing 0.5% Nonidet P-40 and 0.5% deoxycholate or in STE buffer containing 2% Sarkosyl and digested with PK. The blot was incubated with the rabbit-derived $F(ab')_2$ fragment of anti-mouse IgG.

OMPs are heat modifiable and resistant to trypsin (12). In this study, we have confirmed that OMPs of *K. pneumoniae* and *S. typhimurium* were also resistant to PK and the resulting molecules migrated around 37 kDa on SDS-PAGE.

OMPs act as a determinant of the permeability of antimicrobial agents and affect the interaction between bacteria and host defense mechanisms (13). Whereas it is known that the OMPs of *K. pneumoniae* bind to C1q (14), there are no previous reports that indicate the binding between OMPs and IgG. We found that OMPs bound non-specifically to IgG (several kinds of antibodies) during the procedure of Western blot analysis. Because protein A, a cell wall component of *S. aureus*, has been known to bind to the Fc region of IgG (15), we hypothesized that OMPs might also bind to IgG in the same manner. Contrary to our expectations, OMPs still reacted with the $F(ab')_2$ fragment of anti-mouse IgG, indicating that they bound to IgG

in a manner that is different from that of protein A with immunoglobulins. It might be suggested that accidentally acquired antibodies against bacterial OMPs in the serum of immunized animals might react with OMPs, resulting in protease-resistant signals. However, Western blot analysis using anti-mouse IgG produced by a phage-display method, for example, would be required to exclude this hypothesis.

Our findings were not consistent with those of a previous report by Shaked *et al.* (7). They showed that PK-resistant proteins in the urine of patients and animals affected with prion diseases were prion protein and termed them $UPrP^{Sc}$. The signal of $UPrP^{Sc}$ showed a downward shift after PK digestion resulting in a 32-kDa fragment, whereas the majority of PK-resistant signals that we detected did not show a significant downward shift. Apart from the 37-kDa PK-resistant signal, a faint 22-kDa signal was observed in some patients and a 28-kDa signal was observed in both patients and controls. N-terminal sequencing revealed that these signals were fragments of OMPs and PK molecules, respectively. In this study, we did not observe any PK-resistant signals migrating around 32 kDa, which was detected by Shaked *et al.* (7) in the urine of patients. Therefore, the possibility that the PK-resistant molecule in this study might be a different molecule from $UPrP^{Sc}$, as demonstrated by Shaked *et al.* (7), was not excluded.

However, the high incidence of OMPs (37-kDa PK-resistant signals, non-specifically bind to immunoglobulins) in the urine of patients affected with prion diseases, irrespective of the assay conditions, indicated that bacterial contamination would always have to be considered in the application of a "$UPrP^{Sc}$ assay" in the diagnosis of human prion diseases. Our findings suggest that $PrP^{Sc}$ and $PrP^{C}$ may not always exist or could exist at a very low level in urine, and bacterial contamination may often cause false detection of a PK-resistant isoform of prion protein in urine and a misinterpretation of results.

We have also analyzed the urine protein of mice experimentally infected with a prion agent. The PK-resistant signals of 25 kDa were found in the urine of affected mice, but these signals were also detectable using a secondary antibody alone, omitting the labeling by a primary antibody (data not shown). Furthermore, N-terminal sequencing analysis revealed that these PK-resistant signals in mice urine were OMPs of *Pseudomonas aeruginosa*.

In conclusion, the detection of $UPrP^{Sc}$ is not useful or reliable for ante-mortem, definite diagnosis of human prion diseases in the present situation. Further improvement in sensitivity and specificity of this assay may make it a powerful diagnostic tool for prion diseases in the future.

*Acknowledgments*—We thank Dr. Mitsuhiro Tsujihata, Nagasaki North Hospital, Nagasaki, Japan, and Dr. Shunsuke Matsumoto, Second Kawanami Hospital, Fukuoka, Japan, for providing urine samples of the control groups used in this study. We also thank Dr. Mitsuo Takahashi and Dr. Tatsuo Yamada, Department of the Fifth Internal Medicine, Fukuoka University, Japan, for critically reading the manuscript.

REFERENCES

1. World Health Organization (2000) *WHO Infection Control Guidelines for Transmissible Spongiform Encephalopathies: Report of a WHO Consultation, Geneva, Switzerland, 23–26 March 1999*, Section 2.2, Communicable Disease Surveillance and Response (CSR), WHO
2. Demaerel, P., Baert, A. L., Vanopdenbosch, L., Robberecht, W., and Dom, R. (1997) *Lancet* **349**, 847–848
3. Hsich, G., Kenny, K., Gibbs, C. J., Lee, K. H., and Harrington, M. G. (1996) *N. Eng. J. Med.* **335**, 924–930
4. Riemenschneider, M., Wagenpfeil, S., Vanderstichele, H., Otto, M., Wiltfang, J., Kretzschmar, H., Vanmechelen, E., Forstl, H., and Kurz, A. (2003) *Mol. Psychiatry* **8**, 343–347
5. Castellani, R., Parchi, P., Stahl, J., Capellari, S., Cohen, M., and Gambetti, P. (1996) *Neurology* **46**, 1690–1693
6. Bieschke, J., Giese, A., Schulz-Schaeffer, W., Zerr, I., Poser, S., Eigen, M., and Kretzschmar, H. (2000) *Proc. Natl. Acad. Sci. U. S. A.* **97**, 5468–5473
7. Shaked, G. M., Shaked, Y., Kariv-Inbal, Z., Halimi, M., Avraham, I., and Gabizon, R. (2001) *J. Biol. Chem.* **276**, 31479–31482
8. Wilm, M., Shevchenko, A., Houthaeve, T., Breit, S., Schweigerer, L., Fotsis, T., and Mann, M. (1996) *Nature* **379**, 466–469
9. Morgenstern, J. P., Griffith, I. J., Brauer, A. W., Rogers, B. L., Bond, J. F., Chapman, M. D., and Kuo, M. C. (1991) *Proc. Natl. Acad. Sci. U. S. A.* **88**, 9690–9694
10. Hernández-Allés, S., Albertí, S., Álvarez, D., Doménech-Sánchez, A., Martínez-Martínez, L., Gil, J., Tomás, J. M., and Benedí, V. J. (1999) *Microbiology* **145**, 673–679
11. Weiss, M. S., Abele, U., Weckesser, J., Welte, W., Schiltz, E., and Schulz, G. E. (1991) *Science* **254**, 1627–1630
12. Albertí, S., Rodríquez-Quiòones, F., Schirmer, T., Rummel, G., Tomás, J. M., Rosenbusch, J. P., and Benedí, V. J. (1995) *Infect. Immun.* **63**, 903–910
13. Benz, R. (1994) in *Bacterial Cell Walls* (Ghuysen, J.-M., and Hackenbeck, R., eds) pp. 397–424, Elsevier, Amsterdam
14. Albertí, S., Marqués, G., Camprubí, S., Merino, S., Tomás, J. M., Vivanco, F., and Benedí, V. J. (1993) *Infect. Immun.* **61**, 852–860
15. Kessler, S. W. (1975) *J. Immunol.* **115**, 1617–1624